Bioconcentration, bioaccumulation and biomagnification of mercury in plankton of the Mediterranean Sea

Javier Angel Tesán-Onrubia, Lars-Eric Heimbürger-Boavida, Aurélie Dufour, Mireille Harmelin-Vivien, Isabel García-Arévalo, Joël Knoery, Bastien Thomas, François Carlotti, Marc Tedetti, Daniela Bănaru

Bioconcentration, bioaccumulation and biomagnification of mercury in plankton of the Mediterranean Sea

Javier Angel Tesán-Onrubia[a*], Lars-Eric Heimbürger-Boavida[a], Aurélie Dufour[a], Mireille Harmelin-Vivien[a], Isabel García-Arévalo[b], Joël Knoery[b], Bastien Thomas[b], François Carlotti[a], Marc Tedetti[a], Daniela Bănaru[a*]

[a] Aix Marseille Univ, Université de Toulon, CNRS, IRD, MIO UM110, Marseille, France

[b] Ifremer, CCEM Contamination Chimique des Ecosystèmes Marins, F-44311 Nantes, France

* Correspondence:

Javier Angel Tesán-Onrubia; javier.tesan@mio.osupytheas.fr

Daniela Bănaru; daniela.banaru@mio.osupytheas.fr

Lars-Eric Heimbürger-Boavida; lars-eric.heimburger@mio.osupytheas.fr

For submission to Marine Pollution Bulletin – Special issue "Plankton and Contaminants in the Mediterranean Sea: Biological pump and interactions from regional to global approaches"

Revised version

Highlights

- Highest THg bioconcentration was highlighted in picoplankton
- MMHg biomagnified while THg decreased along the plankton food web
- MMHg bioaccumulated and biomagnified in zooplankton
- Highest zooplankton MMHg concentrations were observed in oligotrophic areas

Abstract

Plankton plays a prominent role in the bioaccumulation of mercury (Hg). The MERITE-HIPPOCAMPE campaign was carried out in spring 2019 along a north-south transect including coastal and offshore areas of the Mediterranean Sea. Sampling of sea water and plankton by pumping and nets was carried out in the chlorophyll maximum layer. Two size-fractions of phytoplankton (0.7–2.7 and 2.7–20 µm) and five of zooplankton (between 60

and >2000 μm) were separated, and their total mercury (THg) and monomethylmercury (MMHg) contents were measured. Bioconcentration of THg was significantly higher in the smallest phytoplankton size-fraction dominated by *Synechococcus* spp. The bioaccumulation and biomagnification of MMHg in zooplankton was influenced by size, food sources, biochemical composition and trophic level. MMHg was biomagnified in the plankton food web, while THg decreased toward higher trophic levels. Higher MMHg concentrations were measured in oligotrophic areas. Plankton communities in the Southern Mediterranean Sea had lower MMHg concentrations than those in the Northern Mediterranean Sea. These results highlighted the influence of environmental conditions and trophodynamics on the transfer of Hg in Mediterranean plankton food webs, with implications for higher trophic level consumers.

Keywords

Mercury, methylmercury, plankton, trophic transfer, contamination, food web

1. Introduction

Mercury (Hg), predominantly in its inorganic form, is released to the atmosphere and the ocean from natural and anthropogenic sources, with the latter largely outweighing the former (Outridge et al., 2018). Anthropogenic Hg emissions are thought to have tripled surface ocean Hg levels (Lamborg et al., 2014). Marine apex predator Hg levels are driven by anthropogenic Hg inputs and marine methylmercury (MeHg) production (Medieu et al. 2022), yet their relative importance is still poorly constrained (Wang et al. 2019). The relatively small and semi-enclosed Mediterranean Sea receives proportionally more Hg and the sea water MeHg dynamics are well known, making it an ideal case study (Cossa et al., 2022). Microorganisms present in the ocean can convert inorganic Hg into MeHg species (Villar et al., 2020), namely monomethylmercury (MMHg) and dimethylmercury (DMHg). MMHg is a potent neurotoxic which bioaccumulates in organisms with size and age and biomagnifies in food webs, reaching high concentrations in apex predators (Morel et al., 1998). Mediterranean human populations are exposed to high levels of Hg related to higher marine fish consumption, posing a potential health risk (UNEP, 2019; Petrova et al., 2020). This is further exacerbated by the higher fish Hg levels in the Mediterranean Sea, often exceeding regulatory limits (Aston and Fowler, 1985; Storelli and Marcotrigiano, 2001;

Tseng et al., 2021).

Several hypotheses have been proposed to explain the so-called "Mediterranean Hg anomaly" (Aston and Fowler, 1985; Cossa and Coquery, 2005), mainly attributing the higher biota Hg levels to enhanced MeHg production. The high methylation capacities reported in the Mediterranean Sea may enhance MMHg availability to the lower trophic levels, namely plankton (Cossa and Coquery, 2005, Monperrus et al., 2007; Cossa et al., 2022). Similarly to the Arctic Ocean, the Mediterranean MeHg maxima are located at shallow depths in proximity to the phytoplankton habitat, allowing for an efficient uptake into the food web (Heimbürger et al., 2010, 2015; Cossa et al., 2012). Nevertheless, sea water Hg concentrations alone cannot explain the "Mediterranean Hg anomaly" observed for biota (Aston and Fowler, 1985; Cossa and Coquery, 2005). While Hg concentrations have been extensively observed in Mediterranean higher trophic level biota (Cinnirella et al., 2019 and references therein), only few studies have been conducted on plankton Hg levels (Cossa et al., 2012; Chouvelon et al., 2019).

Although studies are scarce, plankton organisms are hypothesized to play a key role in the accumulation and transfer of Hg in the Mediterranean food webs (Cossa and Coquery, 2005; Harmelin-Vivien et al., 2009; Chouvelon et al., 2018, 2019; Cossa et al., 2022). Phytoplankton bioconcentrates Hg more than 10,000 times from sea water, which is by far the largest enrichment step of Hg along the marine food web (Lee and Fisher, 2016). Mercury bioconcentration has been shown to be related to species and size, with the highest bioconcentration for smallest phytoplankton cells largely driven by their higher surface-to-volume ratio (Lee and Fisher, 2016). In the Mediterranean Sea, phytoplankton is mainly composed of small cells (pico- and nanoplankton) with a low biomass (Leblanc et al., 2018; Boudriga et al., 2022; Tesán-Onrubia et al., 2023), and a high Hg bioconcentration may thus be expected (Chouvelon et al., 2018). In addition, the slow-sinking pico- and nanophytoplankton cells are more prone to remineralization (Guidi et al., 2009) and thus to providing more Hg for methylation (Heimbürger et al., 2010). Due to technical difficulties, data on Hg concentrations in small phytoplankton fractions collected in the field remain scarce to date (Gosnell and Mason, 2015; Gosnell et al., 2017). Zooplankton represents the link between phytoplankton and higher trophic levels. MMHg bioaccumulates in zooplankton with size and age mainly because of food uptake (Tsui and Wang, 2004; Hammerschmidt et al., 2013). A size-based approach has become widely used to study the structure and functioning of the planktonic compartment (Rau et al., 1990; Rolff, 2000;

Carlotti et al., 2008; Hunt et al., 2017). However, taxonomic and groups composition differ between plankton size-fractions (Boudriga et al., 2023; Fierro-González et al., 2023). Zooplankton may exhibit different feeding patterns across size-fractions, ranging from herbivorous to carnivorous, resulting in different Hg exposure (Pućko et al., 2014).

Oligotrophic ecosystems are characterized by lower growth rates, which reduces the biodilution of Hg in biota (i.e., decrease in Hg with increasing biomass) (Silva et al., 2008; Cossa et al., 2012; Chouvelon et al., 2018). The relatively warm waters of the Mediterranean Sea may stimulate Hg-methylating microbes (Bacci et al., 1989; Heimbürger et al. 2010), likewise increase the metabolic activity of higher trophic levels, and reduce excretion rates of MMHg (Remen et al., 2015; Maulvault et al., 2016). The biochemical composition of organisms can influence their physico-chemical affinity for Hg bioaccumulation (Wu and Wang, 2011; Charette et al., 2021). Overall, little is known about the biological mechanisms of accumulation of Hg in plankton in the Mediterranean Sea and the influence of species, size, and biochemical composition of plankton. Moreover, Hg biomagnification in the food web may be related to food sources but also to trophic structure. The longer food web of oligotrophic ecosystems (Décima, 2022; Tesán-Onrubia et al., 2023) may increase MMHg biomagnification (Cossa et al., 2012, 2022). Nevertheless, to date, biomagnification in a size-fractionated plankton food web has, to our knowledge, never been studied.

The Mediterranean Sea represents a semi-enclosed basin with spatial nutrient gradients and different sources and concentrations of Hg in sea water (Durrieu de Madron et al., 2011; Cossa et al., 2022). Spatial variations of Hg concentrations have been shown in both sea water and sediments (Cossa and Martin, 1991; Horvat et al., 1999; Covelli et al., 2001; Tessier et al., 2011; Rosati et al., 2020), potentially impacting Hg concentrations in fishes (Kucuksezgin et al., 2001; Cresson et al., 2015) and at all levels of the food web (Chen et al., 2008). Gosnell and Mason (2015) hypothesized that the spatial variability of Hg concentrations in plankton size-fractions is also related to the plankton productivity. However, in the Mediterranean Sea, no spatially resolved data is available on the Hg content of plankton.

To investigate the "Mediterranean Hg anomaly" at the base of the pelagic food web, sampling different plankton size classes remains a challenge, the main technical difficulty being the collection of large quantities for subsequent chemical analyses. A key feature of the MERITE-HIPPOCAMPE campaign was the implementation of targeted sampling strategies for the collection of large quantities of size-fractionated phyto- and zooplankton at

the chlorophyll maximum layer (CML). Throughout the MERITE-HIPPOCAMPE cruise, samples were taken for sea water, different size-fractions of phyto- (0.7–2.7, 2.7–20 µm) and zooplankton (60–200, 200–500, 500–1000, 1000–2000 and >2000 µm). Complementary studies were also conducted on environmental parameters, species or groups composition, biochemical and stable isotopes composition of the different size-fractions (Boudriga et al., 2022; Fierro-González et al., 2023; Tesán-Onrubia et al., 2023; Tedetti et al., 2023). The aim of our study was to investigate the bioconcentration, bioaccumulation and biomagnification of THg and MMHg in different plankton size classes in contrasted ecoregions of the Mediterranean Sea.

2. Material and methods

2.1 Sampling preparation

The MERITE-HIPPOCAMPE cruise took place in the Mediterranean Sea, between April 13th and May 14th 2019, onboard the R/V *Antea* (Fig. 1; Tedetti and Tronczynski, 2019). A total of 10 stations were sampled in different ecoregions, including coastal sites in the Bay of Marseille and Toulon (France), in the Gulf of Gabès (Tunisia) and offshore Mediterranean waters (Table S1). Details on the sampling sites, the hydro-bio-geochemical context and the sampling techniques are reported in Tedetti et al. (2023).

Unfiltered sea water was collected under trace metal clean conditions with a 12 L GOFLO bottle (General Oceanics). Sea water was filtered through a PFA filter holder (Savillex), holding a 47 mm diameter glass fiber filter of 0.7 µm porosity (GF/F, Whatman), conserved in PFA bottles and immediately analyzed. Suspended particulate matter was sampled using McLane Large Volume Water Transfer System Samplers (WTS6-142LV, 4–8 L min^{-1}), also called *in situ* pumps. These *in situ* pumps were mounted with bulk and sequential filtration systems (Bishop et al., 2012), holding 142 mm diameter nylon (20 µm), GF/D (2.7 µm) and GF/F (0.7 µm) filters, and typically filtered between 169 and 300 L. The glass fiber filters (GF/D and GF/F, Whatman) were pre-combusted (450°C, 6 h), rinsed, dried and weighed prior to deployment. The 20 µm nylon filters (Mougel, France) were cleaned (HCl 0.05% v/v), dried and weighed prior to deployment. After deployment, the filters were stored folded in half in pre-combusted aluminum foil at –20°C.

Zooplankton collection was carried out towing a Multinet Plankton Sampler (Midi type with

0.25 m^2 opening, Hydro-Bios) at ~2 knots. The obtained bulk sample was consecutively sieved to obtain the following fractions: 60–200, 200–500, 500–1000, 1000–2000 and >2000 µm. Samples were stored in cleaned polypropylene tubes and conserved frozen at –20°C. In the laboratory, filters and zooplankton were freeze-dried before being analyzed.

Overall, 67 samples were collected for THg and MMHg measurements in different fractions. We collected 10 samples of sea water, 10 samples of each of the following fractions: 0.7–2.7, 2.7–20, 60–200, 200–500 µm, 9 samples of the 500–1000 µm fraction, 5 samples of the 1000–2000 µm fraction and 3 samples of the >2000 µm fraction.

Dry weight biomass and biochemical content of all the sieved size-fractions were analyzed and are available in Tesán-Onrubia et al. (2023).

2.2 Reagents and standards for Hg analyses

Reagent and standard solutions were prepared in ultrapure water (18 MΩ cm; MilliQ). Sodium tetraethylborate (Merseburger Spezialchemikalien) solution (1% m/v) was prepared in ultrapure water and dispensed into 15 mL trace metal grade polypropylene vials (VWR). The solution was frozen initially and, after thawing, stored at 4°C for up to 3 days. Sodium acetate buffer solution (2 M) was prepared by diluting glacial acetic acid (J.T. Baker) and anhydrous sodium acetate (J.T. Baker), which was muffled at 300°C for 3 h prior to making up the solution. Nitric acid (14 M) and hydrochloric acid (12 M) were bi-distilled in a clean room under trace metal free conditions.

Standard solutions of inorganic Hg (iHg) (0.9 µg L^{-1}) and MMHg (0.02 and 1 µg L^{-1}) for plankton analysis were prepared from standard solutions (NIST3133 for iHg and a 1 µg L^{-1} MMHg solution purchased from Brooks Rand Labs, traceable to NIST3133). The standards were diluted in 0.5% v/v nitric acid and 0.2% v/v hydrochloric acid solution using a precision balance (Mettler Toledo XS105; d = 0.01 mg).

2.3 THg and MMHg in sea water

Filtered dissolved total mercury (dHg) was analyzed on board by cold vapor atomic fluorescence spectrometry (CV-AFS) immediately after sampling. The mineralization of all dissolved Hg species was done using an acidic BrCl solution during 20 to 60 min prior to the analyses. For shipboard analyses, we used a lab-built sample sparging device connected to a

Tekran 2500 fluorescence detector and a chromatography package to quantify fluorescence peaks. For our analyses, a 40 mL aliquot of the digested sample containing its quantitatively oxidized mercury (Hg^{2+}) was placed in a gas-stripping FEP tube. An excess of $SnCl_2$ was added immediately before closing it to convert all Hg into gaseous elemental Hg, Hg(0). The sample was sparged in a FEP tube at 150 mL min^{-1} for 4 min with Hg-free Ar to exsolve Hg(0) and to sweep it toward a gold trap were it was retained. Mercury was thermally desorbed from the trap and swept by an argon stream into the CV-AFS detector. For dHg analyses, the daily 4-point external linear calibration curves were verified with an aliquot of a certified reference material (ORMS-5, National Research Council Canada) that was analyzed every fifth run. Additional 1-point recalibration curves were acquired when the instrument's response drifts by more than 5% from the target value of the reference material. Overall precision and accuracy of dHg measurements, based on repeated analyses of samples, standards and CRMs, was better than 10%, and limits of quantification attained during the cruise were better than 5 pg L^{-1}, based on repeated analyses of 4 pg Hg^{2+}. Unfiltered MeHg species were analyzed back at the laboratory in samples acidified to 0.5% v/v with HCl 11N, and stored in FEP bottles without headspace. Acidification converts the gaseous DMHg to MMHg, and thus the sum of both is measured as MeHg. The general principles of the hydrid generation are as follows. Analyses were carried out by sparging a 40 mL sample aliquot with He while $NaBH_4$ was continuously added (10 g L^{-1} pumped at 0.25 mL min^{-1}). The evolved volatiles were retained on a 20 cm long, U-shaped cryogenic trap and chromatography column (Chromosorb with silicone OV1 at 15%) immersed in liquid nitrogen. When stripping of the MeHg is completed after 7 min, the trap is removed from liquid nitrogen and heated. As it progressively warms, the trapped Hg species including elemental and MeHg are released at different times from the column. Helium and Hg gases exiting from the outlet of the column then flowed through a 20 cm x 1 mm inner diameter quartz tube maintained at 800°C, where Hg species are pyrolyzed to elemental Hg. The cooled helium and Hg vapor were then directed to a mirrored cell (Hellma, Germany) of a CV-AFS detector (Tekran 2500).

A 2-point external calibration was done at the beginning of each day, and after every 5th sample to account for potential instrumental drift. Based on the uncertainty of low amounts of analyte (2 pg Hg as MMHg), the detection limit was 0.29 pg Hg as MMHg, in a 40 mL sample (7 pg L^{-1}). The dissolved methylmercury (dMeHg) species were calculated by subtracting the particulate (0.7 to 20 µm) from the unfiltered fraction.

2.4 THg and MMHg in plankton

THg was analyzed in zooplankton size-fractions (>60 μm) using atomic absorption spectrometry (AAS, AMA 254, LECO). The analyzer was equipped with a low-level Hg optical cell. The certified reference material (MESS-4, National Research Council Canada) was measured at the beginning and end of the run to verify accuracy. The THg measurements were always within the certified values and the limit of detection, corresponding to the blank plus three times the standard deviation, was 23 pg.

In contrast to zooplankton, THg and MMHg on digested filters were simultaneously measured by purge-and-trap gas chromatography pyrolysis atomic fluorescence spectrometry (PT-GC-Pyr-AFS, MERX-M, Brooks Rand Labs) (Sharif et al., 2013). The biomass collected on filters was too low for measuring THg in a subsample with a signal close to the detection limits of the AAS. Secondly, particulate matter may not be evenly distributed in the filters and may not be suitable for subsampling (Bishop et al., 2012).

Filters were digested, and both iHg and MMHg were derivatized and measured simultaneously. Briefly, filters and zooplankton aliquots between 13 and 190 mg were digested in 20 and 60 mL, pre-combusted (350°C, 5 h) glass vials with 4.57 M nitric acid (3.5–15 mL) for 12 h at 60°C (Hammerschmidt and Fitzgerald, 2006). Amber glass vials (60 mL) were filled with ultrapure water and buffered with sodium acetate to pH 4.5–4.9. An aliquot of the acidic extract (400–800 μL) was then added. The solution was spiked with iHg (100 to 400 μL) and MMHg (10 to 400 μL) solutions for quantification *via* standard addition.

Finally, we added the derivatizing agent, sodium tetraethylborate ($NaBeT_4$) and filled the vial with ultrapure water until a slightly negative meniscus was formed. The cap was tightened, and the preparation was gently mixed. The samples were measured by PT-GC-Pyr-AFS. The chromatogram typically contains three peaks, corresponding to different mercury species: elemental mercury (Hg0), ethylmethylHg and diethylHg. THg was calculated as the sum of iHg and MMHg. We followed a standard addition protocol to estimate THg and MMHg concentrations. The low concentrations and matrix effect associated with biological samples make standard addition a more reliable analytical approach than external calibration. For a single sample, five measurements were performed to construct a regression line. Of the five measurements, two corresponded to sample

replicates without addition, and the remaining three to three different volumes of standard solution. The targeted standard volumes corresponded to between 1 and 5 times the amount of iHg or MMHg present in the sample. The linear regression between added iHg or MMHg and the peak height was calculated. The y-intercept of the linear regression was used to obtain the iHg and MMHg concentrations. The correlation coefficients (R^2) ranged from 0.96 to 1.00. The certified reference material (DORM-4, National research council Canada) was digested and measured similarly to the samples. The measurements corresponded respectively to 79 and 85% of the THg and MMHg certified concentrations. The limits of detection for iHg and MMHg were respectively 8 and 0.8 pg.

Based on the measurement made during the MERITE-HIPPOCAMPE cruise between plankton biomass wet and dry weights (% of water in plankton: 90 ± 3%; Tedetti et al., 2023), a factor of 10 was used to allow comparison of the THg and MMHg concentrations expressed here on a dry weight basis, with those reported in the literature. Further experiments were carried out to assess the THg blanks in the filters, which could be due to the retention of dissolved, colloidal and particulate Hg (<0.7 µm) (Table S2). Different volumes of sea water (10–80 L) were filtered as replicates through three stacked 0.7 µm glass fiber filters (GF/F, 142 mm). THg blanks measured on the 2nd and 3rd filters were not significantly different ($H = 1$; $p > 0.05$) and represented less than 2% of the particulate fraction measured on the 1st filter ($n = 12$). We therefore assume that the THg measured on the filters was representative of the particulate fraction, with a negligible contribution of the dissolved (<0.7 µm) fraction.

2.5 Data treatment

The effect of size-fractions and geographical area on the THg, MMHg and fraction of MMHg were assessed by means of one-way ANOVA (F) or non-parametric Kruskal-Wallis (H) tests after testing for normality and homogeneity of variances, followed by appropriate paired comparison tests, using the software Statistica 12. Principal component analysis (PCA) was performed using the R software (R Core Team, 2017). The PCA used data from Tesán-Onrubia et al. (2023) that may influence THg and MMHg in zooplankton: proteins, carbohydrates, lipids, $\delta^{13}C$, $\delta^{15}N$, C/N, THg and MMHg in the 0.7–2.7 and 2.7–20 µm fractions, phytoplankton size-fractions biomass, zooplankton size-fractions biomass, and plankton group composition.

The bioconcentration factor of THg and MMHg (BCF_{Hg}, in L kg^{-1}) was calculated between plankton and sea water:

$$BCF_{Hg} = \left(\frac{[Hg]_{Plankton}}{[Hg]_{Seawater}}\right) \times 10^6$$

where $[Hg]_{Plankton}$ is the dry weight concentrations of THg or MMHg on a given size-fraction (in ng g^{-1}), $[Hg]_{sea\ water}$ is the dissolved concentrations of Hg (dHg) or MeHg (dMeHg) in sea water (in pg L^{-1}), and 10^6 is the unit conversion factor.

The trophic magnification factor (TMF_{Hg}) of THg and MMHg was calculated within the planktonic food web as follows:

$$TMF_{Hg} = 10^a$$

$$\text{Log } [Hg]_{Plankton} = \delta^{15}N * a + b$$

where log $[Hg]_{Plankton}$ is the logarithm of the THg or MMHg concentration in plankton fractions, $\delta^{15}N$ is the nitrogen stable isotope in the plankton fraction and a is the slope of the linear regression.

3. Results and discussion

The basis of marine Mediterranean food webs is mainly constituted of pico- (0.7–2.7 µm) and nanophytoplankton (2.7–20 µm) (Bănaru et al., 2013; 2019). These phytoplankton fractions are consumed by zooplankton (Hunt et al., 2017; Tesán-Onrubia et al., 2023), which transfer the organic matter and the associated contaminants up to higher trophic level consumers. THg and MMHg measurements on the 0.7–2.7 and 2.7–20 µm size-fractions are scarce and were usually only measured on relatively small sea water volumes (Gosnell and Mason, 2015; Gosnell et al., 2017). In the present study, these analyses were performed on large volume samples (>150 L), which enabled precise Hg species measurements and complementary biological and biochemical analyses (Tesán-Onrubia et al., 2023).

3.1 THg and MMHg in phytoplankton

A contrasted pattern of the relationship between concentration and size was observed for THg and MMHg in phyto- and zooplankton size classes (Fig. 2a, 2b, Tables S3, S4). Both THg and

MMHg concentrations decreased in phytoplankton with increasing cell size, but the difference was statistically significant only for THg in the smallest size-fractions (86 ± 32 ng g^{-1} dw in the 0.7–2.7 µm fraction, and 42 ± 28 ng g^{-1} dw in the 2.7–20 µm fraction) ($F = 10.6$, $p = 0.005$). These values were in the upper range (maxima 42–160 ng g^{-1} dw) of previous observations obtained on a wide range of phytoplankton fractions (Baeyens et al., 2003; Hammerschmidt and Fitzgerald, 2006; Beldozska and Kobos, 2018; Cossa et al., 2012; Hammerschmidt et al., 2013; Gosnell and Mason, 2015; Lamborg et al., 2016; Fox et al., 2017; Harding et al., 2018). However, our measurements were lower than the maxima (420–740 ng g^{-1} dw) reported in studies with larger size-fractions (Bargagli et al., 1998), indirect measurements (Luengen and Flegal, 2009), small volumes of filtered sea water (Gosnell et al., 2017) and estuaries (Kehrig et al., 2009; Mason et al., 2021, 2023) (Table S5). Mean MMHg concentrations of 1.2 ± 0.7 ng g^{-1} dw and 0.8 ± 0.6 ng g^{-1} dw were measured in the 0.7–2.7 and in the 2.7–20 µm fractions, respectively, and are within the range of previous studies. Our observations correspond well to MMHg concentration measured in phytoplankton (Baeyens et al., 2003; Hammerschmidt and Fitzgerald, 2006; Luengen and Flegal 2009; Cossa et al., 2012; Hammerschmidt et al., 2013; Gosnell and Mason, 2015; Gosnell et al., 2017; Fox et al., 2017; Harding et al., 2018) but were lower than concentrations modeled for the Mediterranean Sea (2–15 ng g^{-1} dw) (Rosati et al., 2022) and for the global ocean (12–185 ng g^{-1} dw) (Zhang et al., 2020; Wu et al., 2021).

Chouvelon et al. (2019) showed that Hg bioaccumulation in the lowest size-fractions (6–60 µm) may be high compared to larger plankton size-fractions. The higher surface-to-volume ratio (giving a higher contact surface), which increases Hg uptake (Fisher, 1985), may explain the higher concentrations of THg measured in picoplankton in our study. Small phytoplankton cells are prevalent in Mediterranean oligotrophic waters and during our sampling survey (Boudriga et al., 2022). Enhanced concentrations of MeHg have previously been observed in sea water during pico- and nanoplankton blooms in the Mediterranean Sea (Heimbürger et al., 2010).

Low dissolved Hg (dHg) and MMHg (dMHg) concentrations measured in this study (94 ± 32 pg L^{-1} and 13 ± 7 pg L^{-1}, respectively, Table S6) are likely due to enhanced photochemistry and evasion (Cossa et al., 2009; Sunderland et al., 2009; Heimbürger et al., 2010; Cossa et al., 2022). The mean BCF_{THg} values in the 0.7–2.7 and 2.7–20 µm fractions were 2 x 10^6 L kg^{-1} dw and 1 x 10^6 L kg^{-1} dw, respectively, while the mean BCF_{MMHg} values were 1 x 10^5 L kg^{-1} dw and 8 x 10^5 L kg^{-1} dw, respectively (Table S7). Mediterranean phytoplankton of different

size classes bioconcentrate THg and MMHg 10^6 and 10^5 times, respectively, from sea water, these values being in the upper range of those reported in the literature (Table S5). The mean THg bioconcentration values observed in this study are >10 times higher than the partitioning coefficient of suspended particulate matter (K_d), generally used in global THg models (Zhang et al., 2014), which testifies to the need for more accurate regional data. Various studies have already highlighted the underestimation of K_d, constraining Hg export fluxes from the surface and, more broadly, its biogeochemical cycle (Lamborg et al., 2016; Tesán-Onrubia et al., 2020). It has also been observed that MMHg bioconcentration was promoted under low dissolved organic carbon concentrations (Schartup et al., 2018).

The MERITE-HIPPOCAMPE cruise offered a unique opportunity to couple biological and contaminant analyses (Tedetti et al., 2023), and explore for the first time the relationships between the composition of the suspended particles collected, and their THg and MMHg concentrations. Suspended particles collected on filters were a complex mixture of living and dead organisms (autotrophic and heterotrophic), also containing detritus and mineral particles. Tesán-Onrubia et al. (2023) showed that the 0.7–2.7 and 2.7–20 µm size-fractions were dominated (86% of the total biomass) by two phytoplankton groups: *Synechococcus* spp. (~1 µm) and nanoeukaryotes (~4 µm). The two axes of the PCA analysis relating THg and MMHg concentrations to the size class and group composition of phytoplankton explained 56% of the variability (Fig. S1). Higher THg concentrations were associated with a dominance of *Prochlorococcus* spp. (~0.5 µm) in the 0.7–2.7 µm size-fraction, and a dominance of nanoeukaryotes in the 2.7–20 µm size-fraction. Similarly, higher MMHg concentrations were related to the dominance of *Synechococcus* spp. in the 0.7–2.7 µm size-fraction, and to the dominance of *Cryptophyceae* (~6 µm) in the 2.7–20 µm size-fraction. These two phytoplankton size-fractions constitute a large part of the diet of zooplankton organisms between 200 and 1000 µm size, and represent an important source of Hg for consumers (Tesán-Onrubia et al., 2023).

3.2 THg and MMHg in zooplankton

THg and MMHg bioaccumulated with size among zooplankton, their concentrations increasing from 22 to 45 ng g^{-1} dw, and from 3 to 7 ng g^{-1} dw, respectively, in 60 to 2000 µm size-fractions (Fig. 2a, 2b, Tables S3, S4). Bioaccumulation of MMHg with zooplankton size was previously shown in the North Atlantic (Hammerschmidt et al., 2013), while no

difference was found for THg in the Mediterranean (Chouvelon et al., 2019). THg and MMHg concentration values reported here in the Mediterranean zooplankton were comparable to those observed in other regions (Table S8) (Stern and Macdonald, 2005; Hammerschmidt and Fitzgerald, 2006; Loseto et al., 2008; Lavoie et al., 2010; Cossa et al., 2012; Hammerschmidt et al., 2013; Gosnell and Mason, 2015; Gosnell et al., 2017; Harding et al., 2018), but were lower than those from the Arctic Ocean (Campbell et al., 2005; Foster et al., 2012; Pućko et al., 2014; Fox et al., 2017) and from one study in the Mediterranean Sea (Buckman et al., 2018). Our measured MMHg concentrations in zooplankton are in relatively good agreement with model outputs for the Mediterranean Sea (3–10 ng g^{-1} dw) (Rosati et al., 2022) and the global ocean (1–69 ng g^{-1} dw) (Zhang et al., 2020; Wu et al., 2021).

Changes in metabolism during an organism's life cycle may impact its MMHg concentration. Hammerschmidt and Fitzgerald (2006) showed reduced removal and higher uptake rates in large-size organisms compared to smaller ones. Fierro-González et al. (2023) reported an increase in carnivory with increasing size of zooplankton, which was also in agreement with increasing trophic level traced by $\delta^{15}N$ (Tesán-Onrubia et al., 2023). The lowest THg and the highest MMHg concentrations were both measured in the largest size-fraction (>2000 μm) (Table S3, S4 and S9), as observed in previous studies (Chouvelon et al., 2019).

The biochemical composition of zooplankton may also explain the accumulation of THg and particularly MMHg. MMHg concentrations were significantly correlated with particulate organic carbon (POC), proteins and lipids in zooplankton ($R^2 = 0.47$, $p < 0.0001$; $R^2 = 0.18$, $p = 0.009$ and $R^2 = 0.25$, $p = 0.002$, respectively). The quantity of these compounds increased with the size of zooplankton, except for the >2000 μm fraction (Tesan-Onrubia et al., 2023). The affinity of Hg for POC and proteins is due to the capacity of thiol groups present in cellular proteins to effectively bind to Hg and MMHg (Ravichandran, 2004; Yoon et al., 2005; Gosnell and Mason, 2015).

3.3 Trophic transfer of THg and MMHg

Trophic transfer in the plankton food web was assessed taking into consideration all phyto- and zooplankton size-fractions. The two smallest size-fractions of phytoplankton (0.7–2.7 and 2.7–20 μm) presented the highest THg but the lowest MMHg concentrations with respect to most zooplankton size-fractions ($H = 23.9$, $p < 0.0001$ and $H = 30.1$, $p < 0.0001$, respectively) (Fig. 2a, 2b, Tables S3, S4). While THg concentrations were related mainly to the effect of the surface-volume ratio on bioconcentration in phytoplankton, MMHg concentrations were

mainly related to predation relationships and biomagnification processes among zooplankton fractions. Biomagnification was assessed by using the $\delta^{15}N$ as a proxy of trophic level (Fig. 3). The logTHg and logMMHg showed respectively negative and positive correlations with $\delta^{15}N$ ($R^2 = 0.1$, $p < 0.05$ and $R^2 = 0.43$, $p < 0.0001$, respectively, $n = 57$), indicating a bioreduction of THg ($TMF_{THg} = 0.9$) and a biomagnification of MMHg in the food web studied ($TMF_{MMHg} = 1.7$). In our work, particularly low TMF_{THg} were recorded, indicating a marked bioreduction of THg within the planktonic food web. Chouvelon et al. (2009) also observed no THg increase in zooplankton fractions of increasing size, and THg biomagnification in the food web only when zooplanktivorous fishes were considered. In our case, when only zooplankton size-fractions >60 µm were considered, significant positive correlations were observed for both logTHg and logMMHg and $\delta^{15}N$ ($R^2 = 0.22$, $p < 0.005$ and $R^2 = 0.39$, $p < 0.0001$, respectively), thus evidencing the biomagnification of THg ($TMF_{THg} = 1.3$) and a higher biomagnification factor of MMHg ($TMF_{MMHg} = 2.1$).

The high proportions of MMHg, exceeding 95% in higher trophic level consumers (UNEP, 2019), as well as the lack of data in the literature regarding primary producers and particularly pico- and nanoplankton, may explain these differences. The plankton TMF_{MMHg} in our study showed high values compared to other marine food webs, which also included higher trophic level organisms (Atwell et al., 1998; Campbell et al., 2005; Al-Reasi et al., 2007; Nfon et al., 2009; Lavoie et al., 2010, 2013; Cossa et al., 2012; Chouvelon et al., 2018; Harding et al., 2018; Hilgendag et al., 2022). Low growth rates, specific to the oligotrophic Mediterranean Sea, seem to induce higher MMHg biomagnification in planktivorous food webs (Cossa et al., 2012; Chouvelon et al., 2018). The %MMHg significantly increased between phyto- and zooplankton groups from a mean of 3% in the 0.7–20 µm fractions to 23% in the >60 µm fraction ($H = 35.8$, $p < 0.0001$) (Fig. 2c), highlighting the preferred biomagnification of MMHg. Inorganic Hg has a lower assimilation efficiency compared to MMHg, while their efflux rates are similar (Mason et al., 1996; Lawson and Mason, 1998; Lee and Fisher, 2017), explaining the inverted patterns between food sources and consumers. Inorganic Hg reacts in the same way as other trace metals (Chen and Folt, 2000; Ho et al., 2007; Chouvelon et al., 2019; Chifflet et al., 2023). To our knowledge, there is no previous estimation of MMHg biomagnification in plankton food web considering different size-fractions of phyto- and zooplankton. The few studies that have explored this point consisted of models for the Mediterranean Sea (Rosati et al., 2022) and the global ocean (Zhang et al., 2020; Wu et al., 2021). Without exception, these models indicate bioreduction of MMHg in plankton food

webs, mainly composed of herbivorous and omnivorous organisms, and biomagnification when carnivorous organisms were taken into consideration. Our results suggest the contrary, biomagnification of MMHg occurs in all plankton consumers, independently of their trophic position.

The trophic transfer efficiency between phytoplankton (0.7–2.7 and 2.7–20 µm) and zooplankton size-fractions (>60 µm) was assessed by considering the total amounts of THg and MMHg available in their respective biomasses at the CML (Fig. 4). THg amounts in phyto- and zooplankton biomass was 15 and 1 ng m^{-3} of sea water, respectively, while their respective MMHg contents amounted to 200 and 300 pg m^{-3}. MMHg is almost 10 times higher than that modeled in the Mediterranean Sea (Rosati et al., 2022). The trophic transfer efficiency of THg ranged from 2 to 21% (average 8%), while it was higher for MMHg, ranging from 11 to 169 %, with an average of 78%. Zooplankton can represent a comparable or even larger sink of MMHg when compared to phytoplankton. Longer lifespan together with bioaccumulation can lead to a higher MMHg storage in zooplankton despite their lower biomass than phytoplankton. The MMHg trophic transfer efficiency estimated here presented a higher value than the zooplankton daily grazing, which accounted for 2.7 to 27% of the phytoplankton stock (Fierro-González et al., 2023). Considering daily grazing and Hg concentrations in phytoplankton and assuming a quantitative assimilation of MMHg, zooplankton organisms should have grazed for 6 to 13 days to reach the MMHg concentrations measured in their body. This short integration time suggested that zooplankton could be a good bioindicator of Hg exposure over days or a few weeks. The results reported here indicated that MMHg was efficiently biomagnified and transferred along the plankton food web, in contrast to a rather inefficient transfer of inorganic Hg.

3.4 Spatial variability of THg and MMHg

Dissolved Hg (dHg) concentrations ranged from 50 to 165 pg L^{-1} at St11 and St4, respectively. Dissolved MeHg (dMeHg) concentrations ranged from detection limits (7 pg L^{-1}) at St1, St9, St11, St17 and St19 to 26 pg L^{-1} in St3. Both Hg species were comparable to previous studies in the Mediterranean Sea (Jiskra et al., 2021; Cossa et al., 2022).

THg and MMHg concentrations in phytoplankton (0.7–20 µm) showed strong spatial variations in the western Mediterranean, with the highest values in the smallest fraction recorded at St1 (Toulon in the north) and St17 (Gabès in the south) (Table S3 and S4). Volume concentrations of MMHg in the 0.7 to 20 µm fractions (in pg L^{-1}) were significantly

correlated to phytoplankton biomass ($R^2 = 0.49$, $p < 0.001$) (Table S10). This highlighted the influence of the biomass on Hg-uptake at the basis of the plankton food web. Zones with high biomass of small phytoplankton cells may store a large amount of Hg in phytoplankton, bioavailable then for grazers and higher trophic level consumers. In addition, inorganic Hg may represent a substrate for MMHg production.

Our results suggested higher THg and especially MMHg differences in zooplankton between stations than between size-fractions (Fig. 5, Table S3 and S4). The high growth rates and short life cycles of zooplankton make it a potentially relevant biomonitor for ambient MMHg concentrations over short periods, as suggested in the previous section. This observation contrasts with the high variability reported in marine organisms of higher trophic level related in particular to longer life span and larger home ranges (UNEP, 2019).

THg and MMHg concentrations of zooplankton size-fractions available at all stations (60–200, 200–500 and *500–1000 µm, *unavailable for St17) were pooled to test zooplankton spatial variability that appeared higher for MMHg than for THg (Fig. 5). Significant differences were reported between stations only for MMHg ($H = 24.0$, $p = 0.004$). Mean MMHg concentrations differed ten-fold between minimum (0.6 ng g^{-1} dw, St17) and maximum values (9.4 ng g^{-1} dw, St1). This highlighted the importance of measuring MMHg in consumers with lower trophic levels. Zooplankton from northern (St1, 2, 3 and 4) and offshore (St9, 10 and 11) areas presented higher MMHg concentrations than those from the southern area (St15, 17 and 19) ($H = 14.0$, $p = 0.001$). A $TMF_{MMHg} < 1$ indicated a bioreduction of MMHg in zooplankton and consequently a lower exposure to Hg of zooplankton along the Tunisian coast (St17 and 19). (Fig. 6).

The two axes of the PCA analysis, performed between THg, MMHg, POC, C/N, protein, lipids, $\delta^{13}C$, $\delta^{15}N$, and biomass values in zooplankton per station, explained 57% of the variability (Fig. S2). Two groups of stations were observed along the first axis: the first group gathering St1, 2, 9, 10 and 11, and the second one including St3, 4, 15, 17, and 19. The first group was related to high concentrations in POC, proteins, lipids, THg, MMHg, trophic level and $\delta^{15}N$ in zooplankton, while the second group was correlated with high values of C/N, $\delta^{13}C$ and zooplankton biomass. MMHg in zooplankton increased with the trophic level ($\delta^{15}N$ may be used as a proxy). Zooplankton MMHg decreased with increasing amounts of organic matter, likely because of the affinity of POC, proteins and lipids for Hg. MMHg concentrations in zooplankton were high in oligotrophic, low productivity areas with low zooplankton biomass, high trophic level and high POC, protein and lipid content. Under

oligotrophic conditions, zooplankton were limited by food resources and, as a result, their biomass and growth rates decreased, and increasing Hg bioaccumulation was observed. Oligotrophic ecosystems also have longer food webs with intermediate consumers (ciliates, dinoflagellates, microzooplankton, etc.), which may constitute a trophic link between pico- and nanoplankton, and mesozooplankton, generating additional food steps and probably increasing the biomagnification processes (Søreide et al., 2006; Kürten et al., 2013).

The negative correlation in zooplankton between MMHg and its biomass may suggest a biodilution with growth in more productive areas. This is probably the case in the Gulf of Gabès where lower Hg concentrations in planktivorous species were already reported compared to those in the north-western Mediterranean basin (Aboul-Dahab et al., 1986; Ben Hassine et al., 1990; Joiris et al., 1999). Moreover, in ecosystems where nutrients and phytoplankton resources are abundant, herbivory is the main food pathway, generating lower trophic level ecosystems (Sommer et al., 2002) and thus potentially lower Hg concentrations in consumers.

Coastal areas have been considered to be hotspots for Hg-accumulation due to proximity to sediment and resuspension (Chen et al., 2008). Cossa et al. (2018) showed that MeHg concentrations in subsurface waters are higher in Mediterranean offshore waters. Although coastal regions are subjected to additional sources of Hg (submarine groundwater discharge, rivers and sediments), our results evidenced a lower trophic transfer of Hg in plankton food webs compared to offshore areas, as also observed by Cossa et al. (2012) in the Gulf of Lion. There is indeed more and more evidence of *in situ* Hg methylation in oxygenated waters of the open ocean (Mason and Fitzgerald, 1990; Blum et al., 2013; Masbou et al., 2015; Villar et al. 2020; Liu et al., 2021), and the Mediterranean Sea (Cossa et al. 2022).

However, potential sources of Hg in contaminated areas must be considered as well. Toulon Bay represents an important hotspot of Hg, containing large amounts in its sediments (Tessier et al., 2011) and may be responsible for the highest concentrations measured in this study. High concentrations of THg and MMHg have already been recorded in fish and mussels in Toulon Bay (Cresson et al., 2014; Briant et al., 2017).

4. Conclusions

Few Hg data are currently available for plankton, particularly for MMHg, and they generally show wide variations. An inappropriate plankton sampling strategy may lead to the collection

of organisms with a heterogenous size and composition, highly impacting their Hg and MMHg concentrations. We have tried to overcome these limitations with a dedicated sampling strategy for the acquisition of different phyto- and zooplankton size-classes, the acquisition of trophic proxies and the collection of sufficient biomass for complementary biological and chemical analyses.

High THg and MMHg bioconcentration values were observed for phytoplankton, with the highest values for picoplankton. Small phytoplankton cells were the main contributors to primary production in the Mediterranean waters during our sampling campaign and a major food source for zooplankton. Phytoplankton THg concentrations were higher overall compared to the existing literature. Our study implies that phytoplankton in the oligotrophic Mediterranean Sea is an important driver in the biomagnification of MMHg.

Although THg accumulation through diet is a widely accepted process, our results show that THg bioreduces while MMHg bioaccumulates in the plankton food web. Different kinetics of iHg and MMHg have been evidenced in plankton, supporting the need to analyze both phyto- and zooplankton, and to relate them to their species/group composition in future studies.

Biomagnification of MMHg in all plankton consumers was evidenced, independently of their trophic position. High biomagnification factors were measured compared to previous studies, suggesting an effective transfer in Mediterranean plankton food webs.

Moreover, the biochemical composition of zooplankton, particularly the availability of POC, proteins and lipids appears to have an important role in MMHg bioaccumulation.

Spatial variability in MMHg concentrations in zooplankton was important, with ten-fold differences between areas. Productivity gradients may explain these contrasts. Higher zooplankton MMHg concentrations were measured in low productive areas offshore. In contrast, more productive coastal planktonic food webs showed lower zooplankton MMHg concentrations. Our results suggest a lower impact of Hg on plankton food webs in the less poorly-studied southern Mediterranean Sea, but more observations are needed to corroborate this. Oligotrophy and plankton trophodynamics were key factors in the transfer of Hg in the Mediterranean Sea, playing probably an important role in the Hg transfer along food webs. Our study may thus contribute to explaining the higher Hg levels observed in Mediterranean apex predators. The impact of climate change is thought to contribute to the increase of the oligotrophy and the decrease in size of phytoplankton and may thus exacerbate Hg accumulation in Mediterranean marine food webs in the future. Overall, our study suggests that bioconcentration of MMHg into phytoplankton and subsequent bioaccumulation and

biomagnification are by far the most important factors driving higher trophic level MMHg exposure. As such, the efforts in reducing Hg emissions within the Minamata Convention may be outweighed by the effects of climate change on the lower marine food web structure.

Author contribution statement

Conception and design of study: DB, LEHB, FC, MT, JK

Acquisition of data: JATO, JK, BT, MT, FC

Analysis and/or interpretation of data: JATO, DB, LEHB, MHV, MT, AD, BT, JK

Drafting of the manuscript: JATO, DB, LEHB, MHV, MT

Revising/editing of the manuscript: JATO, DB, LEHB, MHV, AD, MVL, IGA, JK, BT, FC, MT

Project administration and funding acquisition: DB, MT, FC

Acknowledgements

The authors wish to thank the crew of the R/V Antea and the various platforms of the Mediterranean Institute of Oceanography which have contributed to the data acquisition: Plateforme Analytique de Chimie des Environnements Marins (PACEM) for the POC/PON measurements, Plateforme Régionale de Cytométrie pour la Microbiologie (PRECYM) for cytometric analyses, Microscopie et Imagerie numérique (MIM) for identification expertise and the Service Atmosphère-Mer (SAM) for the technical and operational tasks. The authors thank the LIENSs joint research unit (CNRS - La Rochelle University) for the measurement of $\delta^{13}C$ and $\delta^{15}N$ values. The MERITE-HIPPOCAMPE project has been funded by the cross-disciplinary Pollution & Contaminants axis of the CNRS-INSU MISTRALS program (joint action of the MERMEX-MERITE and CHARMEX subprograms) and received support from the IRD French-Tunisian International Joint Laboratory (LMI) COSYS-Med. We are grateful for the additional funding received from IFREMER, the MIO Action Sud and Transverse Axis programs (CONTAM Transversal Axis), and from the IRD Ocean Department. This study received funding by the CONTAMPUMP project (ANR JCJC #19-CE34-0001-01). We warmly thank Michael Paul for improvement of the English. Finally, we acknowledge two reviewers for their helpful and constructive comments and suggestions.

Supplementary information

Supplementary material related to this article is available online.

References

Aboul-Dahab, O., Halim, Y. and ElRayis, O.,1986. Mercury species in coastal marine organisms from different trophic levels west of Alexandria. In FAO/UNEP/WHO/IOC/IAEA Meeting on the biogeochemical cycle of mercury in the Mediterranean. FAO Fish Report. No. 325 (suppl), Rome, pp. 1-7.

Al-Reasi, H.A., Ababneh, F.A., Lean, D.R., 2007. Evaluating mercury biomagnification in fish from a tropical marine environment using stable isotopes (δ13C and δ15N). Environmental Toxicology and Chemistry 26, 1572–1581. https://doi.org/10.1897/06-359R.1

Aston, S.R., Fowler, S.W., 1985. Mercury in the open Mediterranean: evidence of contamination? Science of the Total Environment 43, 13–26. https://doi.org/10.1016/0048-9697(85)90028-2

Atwell, L., Hobson, K.A., Welch, H.E., 1998. Biomagnification and bioaccumulation of mercury in an arctic marine food web: insights from stable nitrogen isotope analysis. Canadian Journal of Fisheries and Aquatic Sciences. 55, 1114–1121. https://doi.org/10.1139/f98-001

Bacci, E., 1989. Mercury in the Mediterranean. Marine Pollution Bulletin 20, 59–63. https://doi.org/10.1016/0025-326X(89)90227-0

Baeyens, W., Leermakers, M., Papina, T., Saprykin, A., Brion, N., Noyen, J., De Gieter, M., Elskens, M., Goeyens, L., 2003. Bioconcentration and biomagnification of mercury and methylmercury in North Sea and Scheldt estuary fish. Archives of Environmental Contamination and Toxicology 45, 498–508. https://doi.org/10.1007/s00244-003-2136-4

Bănaru, D., Diaz, F., Verley, P., Campbell, R., Navarro, J., Yohia, C., Oliveros-Ramos, R., Mellon-Duval, C., Shin, Y.-J., 2019. Implementation of an end-to-end model of the Gulf of Lions ecosystem (NW Mediterranean Sea). I. Parameterization, calibration and evaluation. Ecological Modelling 401, 1–19. https://doi.org/10.1016/j.ecolmodel.2019.03.005

Bănaru, D., Mellon-Duval, C., Roos, D., Bigot, J.-L., Souplet, A., Jadaud, A., Beaubrun, P., Fromentin, J.-M., 2013. Trophic structure in the Gulf of Lions marine ecosystem (north-western Mediterranean Sea) and fishing impacts. Journal of Marine Systems 111–112, 45–68. https://doi.org/10.1016/j.jmarsys.2012.09.010

Bargagli, R., Monaci, F., Sanchez-Hernandez, J.C., Cateni, D., 1998. Biomagnification of

mercury in an Antarctic marine coastal food web. Marine Ecology Progress Series 169, 65–76. https://doi.org/10.3354/meps169065

Bełdowska, M., Kobos, J., 2018. The variability of Hg concentration and composition of marine phytoplankton. Environmental Science Pollution Research 25, 30366–30374. https://doi.org/10.1007/s11356-018-2948-4

Ben-Hassine, O. K., Raibaut, A., Ben Souissi, J. and Rousset, L, 1990. Morphologie de Peroderma cylindricum (Heller, 1865), Copépode parasite de la *Sardina pilchardus* (Walbaum, 1792) et quelques aspects de son écologie dans les eaux côtières tunisiennes. Annales des Sciences naturelles, Zoologie Paris 13(11), 9-16.

Bishop, J.K.B., Lam, P.J., Wood, T.J., 2012. Getting good particles: Accurate sampling of particles by large volume in-situ filtration: Getting good particles. Limnology and Oceanography: Methods 10, 681–710. https://doi.org/10.4319/lom.2012.10.681

Blum, J.D., Popp, B.N., Drazen, J.C., Anela Choy, C., Johnson, M.W., 2013. Methylmercury production below the mixed layer in the North Pacific Ocean. Nature Geosciences 6, 879–884. https://doi.org/10.1038/ngeo1918

Boudriga, I., Thyssen, M., Zouari, A., Garcia, N., Tedetti, M., Bel Hassen, M., 2022. Ultraphytoplankton community structure in subsurface waters along a North-South Mediterranean transect. Marine Pollution Bulletin 182, 113977. https://doi.org/10.1016/j.marpolbul.2022.113977

Briant, N., Chouvelon, T., Martinez, L., Brach-Papa, C., Chiffoleau, J., Savoye, N., Sonke, J., Knoery, J., 2017. Spatial and temporal distribution of mercury and methylmercury in bivalves from the French coastline. Marine Pollution Bulletin 114, 1096–1102. https://doi.org/10.1016/j.marpolbul.2016.10.018

Buckman, K.L., Lane, O., Kotnik, J., Bratkic, A., Sprovieri, F., Horvat, M., Pirrone, N., Evers, D.C., Chen, C.Y., 2018. Spatial and taxonomic variation of mercury concentration in low trophic level fauna from the Mediterranean Sea. Ecotoxicology 27, 1341–1352. https://doi.org/10.1007/s10646-018-1986-5

Campbell, L.M., Norstrom, R.J., Hobson, K.A., Muir, D.C.G., Backus, S., Fisk, A.T., 2005. Mercury and other trace elements in a pelagic Arctic marine food web (Northwater Polynya, Baffin Bay). Science of The Total Environment 351–352, 247–263. https://doi.org/10.1016/j.scitotenv.2005.02.043

Carlotti, F., Thibault-Botha, D., Nowaczyk, A., Lefèvre, D., 2008. Zooplankton community structure, biomass and role in carbon fluxes during the second half of a phytoplankton

bloom in the eastern sector of the Kerguelen Shelf (January–February 2005). Deep Sea Research Part II: Topical Studies in Oceanography 55, 720–733. https://doi.org/10.1016/j.dsr2.2007.12.010

Charette, T., Rosabal, M., Amyot, M., 2021. Mapping metal (Hg, As, Se), lipid and protein levels within fish muscular system in two fish species (Striped Bass and Northern Pike). Chemosphere 265, 129036. https://doi.org/10.1016/j.chemosphere.2020.129036

Chen, C.Y., Folt, C.L., 2000. Bioaccumulation and Diminution of Arsenic and Lead in a Freshwater Food Web. Environmental Science & Technology 34, 3878–3884. https://doi.org/10.1021/es991070c

Chen, C., Amirbahman, A., Fisher, N., Harding, G., Lamborg, C., Nacci, D., Taylor, D., 2008. Methylmercury in Marine Ecosystems: Spatial Patterns and Processes of Production, Bioaccumulation, and Biomagnification. EcoHealth 5, 399–408. https://doi.org/10.1007/s10393-008-0201-1

Chifflet, S., Briant, N., Tesán-Onrubia, J.A., Zaaboub, N., Amri, S., Radakovitch, O., Bănaru, D., Tedetti, M., 2023. Distribution and accumulation of trace metal in the planktonic food web of the Mediterranean Sea (MERITE-HIPPOCAMPE campaign). Marine Pollution Bulletin 186, 114384. https://doi.org/10.1016/j.marpolbul.2022.114384.

Chouvelon, T., Cresson, P., Bouchoucha, M., Brach-Papa, C., Bustamante, P., Crochet, S., Marco-Miralles, F., Thomas, B., Knoery, J., 2018. Oligotrophy as a major driver of mercury bioaccumulation in medium-to high-trophic level consumers: A marine ecosystem-comparative study. Environmental Pollution 233, 844–854. https://doi.org/10.1016/j.envpol.2017.11.015

Chouvelon, T., Strady, E., Harmelin-Vivien, M., Radakovitch, O., Brach-Papa, C., Crochet, S., Knoery, J., Rozuel, E., Thomas, B., Tronczynski, J., Chiffoleau, J.-F., 2019. Patterns of trace metal bioaccumulation and trophic transfer in a phytoplankton-zooplankton-small pelagic fish marine food web. Marine Pollution Bulletin 146, 1013–1030. https://doi.org/10.1016/j.marpolbul.2019.07.047

Cinnirella, S., Bruno, D.E., Pirrone, N., Horvat, M., Živković, I., Evers, D.C., Johnson, S., Sunderland, E.M., 2019. Mercury concentrations in biota in the Mediterranean Sea, a compilation of 40 years of surveys. Scientific Data 6, 205. https://doi.org/10.1038/s41597-019-0219-y

Cossa, D., Martin, J.-M., 1991. Mercury in the Rhône delta and adjacent marine areas. Marine Chemistry, Reactivity of Chemical Species in Aquatic Environments 36, 291–302.

https://doi.org/10.1016/S0304-4203(09)90067-6

Cossa, D., Coquery, M., 2005. The Mediterranean Mercury Anomaly, a Geochemical or a BiologocalIssue, in: Saliot, A. (Ed.), The Mediterranean Sea. Springer Berlin Heidelberg, Berlin, Heidelberg, pp. 177–208. https://doi.org/10.1007/b107147

Cossa, D., Averty, B., Pirrone, N., 2009. The origin of methylmercury in open Mediterranean waters. Limnology and Oceanography 54, 837–844. https://doi.org/10.4319/lo.2009.54.3.0837

Cossa, D., Harmelin-Vivien, M., Mellon-Duval, C., Loizeau, V., Averty, B., Crochet, S., Chou, L., Cadiou, J.-F., 2012. Influences of Bioavailability, Trophic Position, and Growth on Methylmercury in Hakes (*Merluccius merluccius*) from Northwestern Mediterranean and Northeastern Atlantic. Environmental Science & Technology 46, 4885–4893. https://doi.org/10.1021/es204269w

Cossa, D., Knoery, J., Bănaru, D., Harmelin-Vivien, M., Sonke, J.E., Hedgecock, I.M., Bravo, A.G., Rosati, G., Canu, D., Horvat, M., Sprovieri, F., Pirrone, N., Heimbürger-Boavida, L.-E., 2022. Mediterranean Mercury Assessment 2022: An Updated Budget, Health Consequences, and Research Perspectives. Environmental Science & Technology 56, 3840–3862. https://doi.org/10.1021/acs.est.1c03044

Covelli, S., Faganeli, J., Horvat, M., Brambati, A., 2001. Mercury contamination of coastal sediments as the result of long-term cinnabar mining activity (Gulf of Trieste, northern Adriatic sea). Applied Geochemistry 16, 541–558.

Cresson, P., Bouchoucha, M., Miralles, F., Elleboode, R., Mahé, K., Marusczak, N., Thebault, H., Cossa, D., 2015. Are red mullet efficient as bio-indicators of mercury contamination? A case study from the French Mediterranean. Marine Pollution Bulletin 91, 191–199. https://doi.org/10.1016/j.marpolbul.2014.12.005

Cresson, P., Fabri, M.C., Bouchoucha, M., Brach Papa, C., Chavanon, F., Jadaud, A., Knoery, J., Miralles, F., Cossa, D., 2014. Mercury in organisms from the Northwestern Mediterranean slope: Importance of food sources. Science of The Total Environment 497–498, 229–238. https://doi.org/10.1016/j.scitotenv.2014.07.069

Décima, M., 2022. Zooplankton trophic structure and ecosystem productivity. Marine Ecology Progress Series 692, 23–42. https://doi.org/10.3354/meps14077

Di Beneditto, A.P.M., Bittar, V.T., Camargo, P.B., Rezende, C.E., Kehrig, H.A., 2012. Mercury and Nitrogen Isotope in a Marine Species from a Tropical Coastal Food Web. Archives of Environmental Contamination and Toxicology 62, 264–271.

https://doi.org/10.1007/s00244-011-9701-z

Durrieu de Madron, X., Guieu, C., Sempéré, R., Conan, P., Cossa, D., D'Ortenzio, F., Estournel, C., Gazeau, F., Rabouille, C., Stemmann, L., Bonnet, S., Diaz, F., Koubbi, P., Radakovitch, O., Babin, M., Baklouti, M., Bancon-Montigny, C., Belviso, S., Bensoussan, N., Bonsang, B., Bouloubassi, I., Brunet, C., Cadiou, J.-F., Carlotti, F., Chami, M., Charmasson, S., Charrière, B., Dachs, J., Doxaran, D., Dutay, J.-C., Elbaz-Poulichet, F., Eléaume, M., Eyrolles, F., Fernandez, C., Fowler, S., Francour, P., Gaertner, J.C., Galzin, R., Gasparini, S., Ghiglione, J.-F., Gonzalez, J.-L., Goyet, C., Guidi, L., Guizien, K., Heimbürger, L.-E., Jacquet, S.H.M., Jeffrey, W.H., Joux, F., Le Hir, P., Leblanc, K., Lefèvre, D., Lejeusne, C., Lemé, R., Loÿe-Pilot, M.-D., Mallet, M., Méjanelle, L., Mélin, F., Mellon, C., Mérigot, B., Merle, P.-L., Migon, C., Miller, W.L., Mortier, L., Mostajir, B., Mousseau, L., Moutin, T., Para, J., Pérez, T., Petrenko, A., Poggiale, J.-C., Prieur, L., Pujo-Pay, M., Pulido-Villena, Raimbault, P., Rees, A.P., Ridame, C., Rontani, J.-F., Ruiz Pino, D., Sicre, M.A., Taillandier, V., Tamburini, C., Tanaka, T., Taupier-Letage, I., Tedetti, M., Testor, P., Thébault, H., Thouvenin, B., Touratier, F., Tronczynski, J., Ulses, C., Van Wambeke, F., Vantrepotte, V., Vaz, S., Verney, R., 2011. Marine ecosystems' responses to climatic and anthropogenic forcings in the Mediterranean. Progress in Oceanography 91, 97–166. https://doi.org/10.1016/j.pocean.2011.02.003

Fierro-González, P., Pagano, M., Guilloux, L., Makhlouf, N., Tedetti, M., Carlotti, F., 2023. Zooplankton biomass, size structure, and associated metabolic fluxes with focus on its roles at the chlorophyll maximum layer during the plankton-contaminant MERITE-HIPPOCAMPE cruise. Marine Pollution Bulletin 193, 115056. https://doi.org/10.1016/j.marpolbul.2023.115056

Fisher, N.S., 1985. Accumulation of metals by marine picoplankton. Marine Biology 87, 137–142. https://doi.org/10.1007/BF00539421

Foster, K.L., Stern, G.A., Pazerniuk, M.A., Hickie, B., Walkusz, W., Wang, F., Macdonald, R.W., 2012. Mercury Biomagnification in Marine Zooplankton Food Webs in Hudson Bay. Environmental Science & Technology 46, 12952–12959. https://doi.org/10.1021/es303434p

Fox, A.L., Trefry, J.H., Trocine, R.P., Dunton, K.H., Lasorsa, B.K., Konar, B., Ashjian, C.J., Cooper, L.W., 2017. Mercury biomagnification in food webs of the northeastern Chukchi Sea, Alaskan Arctic. Deep Sea Research Part II: Topical Studies in

Oceanography, 144, 63–77. https://doi.org/10.1016/j.dsr2.2017.04.020

Gosnell, K.J., Balcom, P.H., Tobias, C.R., Gilhooly III, W.P., Mason, R.P., 2017. Spatial and temporal trophic transfer dynamics of mercury and methylmercury into zooplankton and phytoplankton of Long Island Sound. Limnology and Oceanography 62, 1122–1138. https://doi.org/10.1002/lno.10490

Gosnell, K.J., Mason, R.P., 2015. Mercury and methylmercury incidence and bioaccumulation in plankton from the central Pacific Ocean. Marine Chemistry 177, 772–780. https://doi.org/10.1016/j.marchem.2015.07.005

Guidi, L., Stemmann, L., Jackson, G.A., Ibanez, F., Claustre, H., Legendre, L., Picheral, M., Gorskya, G., 2009. Effects of phytoplankton community on production, size, and export of large aggregates: A world-ocean analysis. Limnology and Oceanography 54, 1951–1963. https://doi.org/10.4319/lo.2009.54.6.1951

Hammerschmidt, C.R., Finiguerra, M.B., Weller, R.L., Fitzgerald, W.F., 2013. Methylmercury Accumulation in Plankton on the Continental Margin of the Northwest Atlantic Ocean. Environmental Science & Technology 47, 3671–3677. https://doi.org/10.1021/es3048619

Hammerschmidt, C.R., Fitzgerald, W.F., 2006. Bioaccumulation and Trophic Transfer of Methylmercury in Long Island Sound. Archives of Environmental Contamination and Toxicology 51, 416–424. https://doi.org/10.1007/s00244-005-0265-7

Harding, G., Dalziel, J., Vass, P., 2018. Bioaccumulation of methylmercury within the marine food web of the outer Bay of Fundy, Gulf of Maine. PLOS ONE 13, e0197220. https://doi.org/10.1371/journal.pone.0197220

Harmelin-Vivien, M., Cossa, D., Crochet, S., Bănaru, D., Letourneur, Y., Mellon-Duval, C., 2009. Difference of mercury bioaccumulation in red mullets from the north-western Mediterranean and Black seas. Marine Pollution Bulletin 58, 679–685. https://doi.org/10.1016/j.marpolbul.2009.01.004

Heimbürger, L.-E., Cossa, D., Marty, J.-C., Migon, C., Averty, B., Dufour, A., Ras, J., 2010. Methyl mercury distributions in relation to the presence of nano- and picophytoplankton in an oceanic water column (Ligurian Sea, North-western Mediterranean). Geochimica et Cosmochimica Acta 74, 5549–5559. https://doi.org/10.1016/j.gca.2010.06.036

Heimbürger, L.-E., Sonke, J.E., Cossa, D., Point, D., Lagane, C., Laffont, L., Galfond, B.T., Nicolaus, M., Rabe, B., van der Loeff, M.R., 2015. Shallow methylmercury production in the marginal sea ice zone of the central Arctic Ocean. Scientific Reports 5.

822 https://doi.org/10.1038/srep10318

823 Hilgendag, I.R., Swanson, H.K., Lewis, C.W., Ehrman, A.D., Power, M., 2022. Mercury
824 biomagnification in benthic, pelagic, and benthopelagic food webs in an Arctic marine
825 ecosystem. Science of The Total Environment 841, 156424.
826 https://doi.org/10.1016/j.scitotenv.2022.156424

827 Ho, T.-Y., Wen, L.-S., You, C.-F., Lee, D.-C., 2007. The trace metal composition of size-
828 fractionated plankton in the South China Sea: Biotic versus abiotic sources. Limnology
829 and Oceanography 52, 1776–1788. https://doi.org/10.4319/lo.2007.52.5.1776

830 Horvat, M., Covelli, S., Faganeli, J., Logar, M., Mandić, V., Rajar, R., Širca, A., Žagar, D., 1999.
831 Mercury in contaminated coastal environments; a case study: the Gulf of Trieste.
832 Science of the Total Environment 237, 43–56.

833 Hunt, B.P.V., Carlotti, F., Donoso, K., Pagano, M., D'Ortenzio, F., Taillandier, V., Conan, P.,
834 2017. Trophic pathways of phytoplankton size classes through the zooplankton food
835 web over the spring transition period in the north-west Mediterranean Sea. Journal of
836 Geophysical Research: Oceans 122, 6309–6324. https://doi.org/10.1002/2016JC012658

837 Jiskra, M., Heimbürger-Boavida, L.-E., Desgranges, M.-M., Petrova, M.V., Dufour, A., Ferreira-
838 Araujo, B., Masbou, J., Chmeleff, J., Thyssen, M., Point, D., Sonke, J.E., 2021.
839 Mercury stable isotopes constrain atmospheric sources to the ocean. Nature 597, 678–
840 682. https://doi.org/10.1038/s41586-021-03859-8

841 Joiris, C.R, Holsbeek, L., Laroussi moatemri, N., 1999. Total and Methylmercury in Sardines
842 Sardinella aurita and Sardina pilchardus from Tunisia. Marine Pollution Bulletin 38,
843 188–192. https://doi.org/10.1016/S0025-326X(98)00171-4

844 Kehrig, H.A., Palermo, E.F.A., Seixas, T.G., Branco, C.W.C., Moreira, I., Malm, O., 2009.
845 Trophic transfer of methylmercury and trace elements by tropical estuarine seston and
846 plankton. Estuarine, Coastal and Shelf Science 85, 36–44.
847 https://doi.org/10.1016/j.ecss.2009.05.027

848 Kucuksezgin, F., Altay, O., Uluturhan, E., Kontas, A., 2001. Trace Metal and Organochlorine
849 Residue Levels in Red Mullet (*Mullus barbatus*) from the Eastern Aegean, Turkey.
850 Water Research 35, 2327–2332. https://doi.org/10.1016/S0043-1354(00)00504-2

851 Kürten, B., Painting, S.J., Struck, U., Polunin, N.V.C., Middelburg, J.J., 2013. Tracking seasonal
852 changes in North Sea zooplankton trophic dynamics using stable isotopes.
853 Biogeochemistry 113, 167–187. https://doi.org/10.1007/s10533-011-9630-y

854 Lamborg, C.H., Hammerschmidt, C.R., Bowman, K.L., Swarr, G.J., Munson, K.M., Ohnemus,

D.C., Lam, P.J., Heimbürger, L.-E., Rijkenberg, M.J.A., Saito, M.A., 2014. A global ocean inventory of anthropogenic mercury based on water column measurements. Nature 512, 65–68. https://doi.org/10.1038/nature13563

Lamborg, C.H., Hammerschmidt, C.R., Bowman, K.L., 2016. An examination of the role of particles in oceanic mercury cycling. Philosophical Transactions of the Royal Society A 374, 20150297. https://doi.org/10.1098/rsta.2015.0297

Lavoie, R.A., Hebert, C.E., Rail, J.-F., Braune, B.M., Yumvihoze, E., Hill, L.G., Lean, D.R.S., 2010. Trophic structure and mercury distribution in a Gulf of St. Lawrence (Canada) food web using stable isotope analysis. Science of The Total Environment 408, 5529–5539. https://doi.org/10.1016/j.scitotenv.2010.07.053

Lavoie, R.A., Jardine, T.D., Chumchal, M.M., Kidd, K.A., Campbell, L.M., 2013. Biomagnification of Mercury in Aquatic Food Webs: A Worldwide Meta-Analysis. Environmental Science & Technology. 47, 13385–13394. https://doi.org/10.1021/es403103t

Lawson, N.M., Mason, R.P., 1998. Accumulation of mercury in estuarine food chains. Biogeochemistry 40, 235–247. https://doi.org/10.1023/A:1005959211768

Leblanc, K., Quéguiner, B., Diaz, F., Cornet, V., Michel-Rodriguez, M., Durrieu de Madron, X., Bowler, C., Malviya, S., Thyssen, M., Grégori, G., Rembauville, M., Grosso, O., Poulain, J., de Vargas, C., Pujo-Pay, M., Conan, P., 2018. Nanoplanktonic diatoms are globally overlooked but play a role in spring blooms and carbon export. Nature Communications 9, 953. https://doi.org/10.1038/s41467-018-03376-9

Lee, C.-S., Fisher, N.S., 2016. Methylmercury uptake by diverse marine phytoplankton. Limnology and Oceanography 61, 1626–1639. https://doi.org/10.1002/lno.10318

Lee, C.-S., Fisher, N.S., 2017. Bioaccumulation of methylmercury in a marine copepod. Environmental Toxicology and Chemistry 36, 1287–1293. https://doi.org/10.1002/etc.3660

Liu, M., Zhang, Q., Maavara, T., Liu, S., Wang, X., Raymond, P.A., 2021. Rivers as the largest source of mercury to coastal oceans worldwide. Nature Geosciences. 14, 672–677. https://doi.org/10.1038/s41561-021-00793-2

Loseto, L.L., Stern, G.A., Deibel, D., Connelly, T.L., Prokopowicz, A., Lean, D.R.S., Fortier, L., Ferguson, S.H., 2008. Linking mercury exposure to habitat and feeding behaviour in Beaufort Sea beluga whales. Journal of Marine Systems, 74, 1012–1024. https://doi.org/10.1016/j.jmarsys.2007.10.004

Luengen, A.C., Russell Flegal, A., 2009. Role of phytoplankton in mercury cycling in the San Francisco Bay estuary. Limnology and Oceanography 54, 23–40. https://doi.org/10.4319/lo.2009.54.1.0023

Masbou, J., Point, D., Guillou, G., Sonke, J.E., Lebreton, B., Richard, P., 2015. Carbon Stable Isotope Analysis of Methylmercury Toxin in Biological Materials by Gas Chromatography Isotope Ratio Mass Spectrometry. Analytical Chemistry 87, 11732–11738. https://doi.org/10.1021/acs.analchem.5b02918

Mason, R.P., Fitzgerald, W.F., 1990. Alkylmercury species in the equatorial Pacific. Nature 347, 457–459. https://doi.org/10.1038/347457a0

Mason, R.P., Reinfelder, J.R., Morel, F.M.M., 1996. Uptake, Toxicity, and Trophic Transfer of Mercury in a Coastal Diatom. Environmental Science & Technology 30, 1835–1845. https://doi.org/10.1021/es950373d

Mason, R.P., 2021. Coastal Phytoplankton and Mercury Dynamics in Watersheds Along the U.S. East Coast From New Jersey to Maine Assessed Using Particulate and Dissolved Samples Collected in 2015 and 2016. Biological and Chemical Oceanography Data Management Office (BCO-DMO).

Mason, R.P., Buckman, K.L., Seelen, E.A., Taylor, V.F., Chen, C.Y., 2023. An examination of the factors influencing the bioaccumulation of methylmercury at the base of the estuarine food web. Science of The Total Environment 886, 163996. https://doi.org/10.1016/j.scitotenv.2023.163996

Maulvault, A.L., Custódio, A., Anacleto, P., Repolho, T., Pousão, P., Nunes, M.L., Diniz, M., Rosa, R., Marques, A., 2016. Bioaccumulation and elimination of mercury in juvenile seabass (*Dicentrarchus labrax*) in a warmer environment. Environmental Research 149, 77–85. https://doi.org/10.1016/j.envres.2016.04.035

Médieu, A., Point, D., Itai, T., Angot, H., Buchanan, P.J., Allain, V., Fuller, L., Griffiths, S., Gillikin, D.P., Sonke, J.E., Heimbürger-Boavida, L.-E., Desgranges, M.-M., Menkes, C.E., Madigan, D.J., Brosset, P., Gauthier, O., Tagliabue, A., Bopp, L., Verheyden, A., Lorrain, A., 2022. Evidence that Pacific tuna mercury levels are driven by marine methylmercury production and anthropogenic inputs. Proceedings of the National Academy of Sciences 119, e2113032119. https://doi.org/10.1073/pnas.2113032119

Monperrus, M., Tessier, E., Amouroux, D., Leynaert, A., Huonnic, P., Donard, O.F.X., 2007. Mercury methylation, demethylation and reduction rates in coastal and marine surface waters of the Mediterranean Sea. Marine Chemistry 107, 49–63.

https://doi.org/10.1016/j.marchem.2007.01.018

Morel, F.M.M., Kraepiel, A.M.L., Amyot, M., 1998. The Chemical Cycle and Bioaccumulation of Mercury. Annual Review of Ecology and Systematics 29, 543–566. https://doi.org/10.1146/annurev.ecolsys.29.1.543

Nfon, E., Cousins, I.T., Järvinen, O., Mukherjee, A.B., Verta, M., Broman, D., 2009. Trophodynamics of mercury and other trace elements in a pelagic food chain from the Baltic Sea. Science of The Total Environment 407, 6267–6274. https://doi.org/10.1016/j.scitotenv.2009.08.032

Outridge, P.M., Mason, R.P., Wang, F., Guerrero, S., Heimbürger-Boavida, L.E., 2018. Updated Global and Oceanic Mercury Budgets for the United Nations Global Mercury Assessment 2018. Environmental Science & Technology 52, 11466–11477. https://doi.org/10.1021/acs.est.8b01246

Petrova, M.V., Ourgaud, M., Boavida, J.R.H., Dufour, A., Tesán Onrubia, J.A., Lozingot, A., Heimbürger-Boavida, L.-E., 2020. Human mercury exposure levels and fish consumption at the French Riviera. Chemosphere 258, 127232. https://doi.org/10.1016/j.chemosphere.2020.127232

Pućko, M., Burt, A., Walkusz, W., Wang, F., Macdonald, R.W., Rysgaard, S., Barber, D.G., Tremblay, J.-é., Stern, G.A., 2014. Transformation of Mercury at the Bottom of the Arctic Food Web: An Overlooked Puzzle in the Mercury Exposure Narrative. Environmental Science & Technology 48, 7280–7288. https://doi.org/10.1021/es404851b

Rau, G., Teyssie, J., Rassoulzadegan, F., Fowler, S., 1990. C-13/C-12 and N-15/N-14 variations among size-fractionated marine particles - implications for their origin and trophic relationships. Marine Ecology Progress Series 7.

Ravichandran, M., 2004. Interactions between mercury and dissolved organic matter—a review. Chemosphere 55, 319–331. https://doi.org/10.1016/j.chemosphere.2003.11.011

R Core Team, 2013. R: A Language and Environment for Statistical Computing. R Foundation for Statistical Computing, Vienna.

Remen, M., Nederlof, M.A.J., Folkedal, O., Thorsheim, G., Sitjà-Bobadilla, A., Pérez-Sánchez, J., Oppedal, F., Olsen, R.E., 2015. Effect of temperature on the metabolism, behaviour and oxygen requirements of *Sparus aurata*. Aquaculture Environment Interactions 7, 115–123. https://doi.org/10.3354/aei00141

Rolff, C., 2000. Seasonal variation in δ13C and δ15N of size-fractionated plankton at a coastal

station in the northern Baltic proper. Marine Ecology Progress Series 203, 47–65. https://doi.org/10.3354/meps203047

Rosati, G., Solidoro, C., Canu, D., 2020. Mercury dynamics in a changing coastal area over industrial and postindustrial phases: Lessons from the Venice Lagoon. Science of The Total Environment 743, 140586. https://doi.org/10.1016/j.scitotenv.2020.140586

Rosati, G., Canu, D., Lazzari, P., Solidoro, C., 2022. Assessing the spatial and temporal variability of methylmercury biogeochemistry and bioaccumulation in the Mediterranean Sea with a coupled 3D model. Biogeosciences 19, 3663–3682. https://doi.org/10.5194/bg-19-3663-2022

Schartup, A.T., Qureshi, A., Dassuncao, C., Thackray, C.P., Harding, G., Sunderland, E.M., 2018. A Model for Methylmercury Uptake and Trophic Transfer by Marine Plankton. Environmental Science & Technology 52, 654–662. https://doi.org/10.1021/acs.est.7b03821

Sharif, A., Monperrus, M., Tessier, E., Amouroux, D., 2013. Determination of methyl mercury and inorganic mercury in natural waters at the pgL−1 level: Intercomparison between PT-GC-Pyr-AFS and GC-ICP-MS using Ethylation or Propylation derivatization. E3S Web of Conferences 1, 09001. https://doi.org/10.1051/e3sconf/20130109001

Silva, A., Carrera, P., Massé, J., Uriarte, A., Santos, M.B., Oliveira, P.B., Soares, E., Porteiro, C., Stratoudakis, Y., 2008. Geographic variability of sardine growth across the northeastern Atlantic and the Mediterranean Sea. Fisheries Research 90, 56–69. https://doi.org/10.1016/j.fishres.2007.09.011

Sommer, U., Stibor, H., Katechakis, A., Sommer, F., Hansen, T., 2002. Pelagic food web configurations at different levels of nutrient richness and their implications for the ratio fish production:primary production, in: Vadstein, O., Olsen, Y. (Eds.), Sustainable Increase of Marine Harvesting: Fundamental Mechanisms and New Concepts. Springer Netherlands, Dordrecht, pp. 11–20. https://doi.org/10.1007/978-94-017-3190-4_2

Søreide, J.E., Hop, H., Carroll, M.L., Falk-Petersen, S., Hegseth, E.N., 2006. Seasonal food web structures and sympagic–pelagic coupling in the European Arctic revealed by stable isotopes and a two-source food web model. Progress in Oceanography 71, 59–87. https://doi.org/10.1016/j.pocean.2006.06.001

Stern, G.A., Macdonald, R.W., 2005. Biogeographic Provinces of Total and Methyl Mercury in Zooplankton and Fish from the Beaufort and Chukchi Seas: Results from the SHEBA Drift. Environmental Science & Technology 39, 4707–4713.

https://doi.org/10.1021/es0482278

Storelli, M.M., Marcotrigiano, G.O., 2001. Total mercury levels in muscle tissue of swordfish (*Xiphias gladius*) and bluefin tuna (*Thunnus thynnus*) from the Mediterranean Sea (Italy). Journal of Food Protection 64, 1058–1061. https://doi.org/10.4315/0362-028x-64.7.1058

Sunderland, E.M., Krabbenhoft, D.P., Moreau, J.W., Strode, S.A., Landing, W.M., 2009. Mercury sources, distribution, and bioavailability in the North Pacific Ocean: Insights from data and models. Global Biogeochemical Cycles 23. https://doi.org/10.1029/2008GB003425

Tedetti, M., Tronczynski, J., 2019. HIPPOCAMPE Cruise. RV Antea. https://doi.org/10.17600/18000900.

Tedetti, M., Tronczynski, J., Carlotti, F., Pagano, M., Ismail, S.B., Sammari, C., Hassen, M.B., Desboeufs, K., Poindron, C., Chifflet, S., Zouari, A.B., Abdennadher, M., Amri, S., Bănaru, D., Abdallah, L.B., Bhairy, N., Boudriga, I., Bourin, A., Brach-Papa, C., Briant, N., Cabrol, L., Chevalier, C., Chouba, L., Coudray, S., Yahia, M.N.D., de Garidel-Thoron, T., Dufour, A., Dutay, J.-C., Espinasse, B., Fierro-González, P., Fornier, M., Garcia, N., Giner, F., Guigue, C., Guilloux, L., Hamza, A., Heimbürger-Boavida, L.-E., Jacquet, S., Knoery, J., Lajnef, R., Belkahia, N.M., Malengros, D., Martinot, P.L., Bosse, A., Mazur, J.-C., Meddeb, M., Misson, B., Pringault, O., Quéméneur, M., Radakovitch, O., Raimbault, P., Ravel, C., Rossi, V., Rwawi, C., Hlaili, A.S., Tesán-Onrubia, J.A., Thomas, B., Thyssen, M., Zaaboub, N., Garnier, C., 2023. Contamination of planktonic food webs in the Mediterranean Sea: Setting the frame for the MERITE-HIPPOCAMPE oceanographic cruise (spring 2019). Marine Pollution Bulletin 189, 114765. https://doi.org/10.1016/j.marpolbul.2023.114765

Tesán-Onrubia, J.A., Petrova, M.V., Puigcorbé, V., Black, E.E., Valk, O., Dufour, A., Hamelin, B., Buesseler, K.O., Masqué, P., Le Moigne, F.A.C., Sonke, J.E., Rutgers van der Loeff, M., Heimbürger-Boavida, L.-E., 2020. Mercury Export Flux in the Arctic Ocean Estimated from 234 Th/ 238 U Disequilibria. ACS Earth and Space Chemistry. https://doi.org/10.1021/acsearthspacechem.0c00055

Tesán-Onrubia, J.A., Tedetti, M., Carlotti, F., Tenaille, M., Guilloux, L., Pagano, M., Lebreton, B., Guillou, G., Fierro-González, P., Guigue, C., Chifflet, S., Garcia, T., Boudriga, I., Belhassen, M., Zouari, A.B., Bănaru, D., 2023. Spatial variations of biochemical content and stable isotope ratios of size-fractionated plankton in the Mediterranean Sea

(MERITE-HIPPOCAMPE campaign). Marine Pollution Bulletin 189, 114787. https://doi.org/10.1016/j.marpolbul.2023.114787

Tessier, E., Garnier, C., Mullot, J.-U., Lenoble, V., Arnaud, M., Raynaud, M., Mounier, S., 2011. Study of the spatial and historical distribution of sediment inorganic contamination in the Toulon bay (France). Marine Pollution Bulletin 62, 2075–2086. https://doi.org/10.1016/j.marpolbul.2011.07.022

Tseng, C.-M., Ang, S.-J., Chen, Y.-S., Shiao, J.-C., Lamborg, C.H., He, X., Reinfelder, J.R., 2021. Bluefin tuna reveal global patterns of mercury pollution and bioavailability in the world's oceans. Proceedings of the National Academy of Sciences 118. https://doi.org/10.1073/pnas.2111205118

Tsui, M.T.K., Wang, W.-X., 2004. Uptake and elimination routes of inorganic mercury and methylmercury in Daphnia magna. Environmental Science & Technology 38, 808–816. https://doi.org/10.1021/es034638x

UN-Environment. Global Mercury Assessment 2018. United Nation Environmental Programme, Chemicals and Health Branch, Programme Chemicals and Health Branch Geneva Switzerland, 2019; www.unenvironment.org/resources/publication/global-mercuryassessment-2018.

Villar, E., Cabrol, L., Heimbürger-Boavida, L.-E., 2020. Widespread microbial mercury methylation genes in the global ocean. Environmental Microbiology Reports 12, 277–287. https://doi.org/10.1111/1758-2229.12829

Wang, F., Outridge, P.M., Feng, X., Meng, B., Heimbürger-Boavida, L.-E., Mason, R.P., 2019. How closely do mercury trends in fish and other aquatic wildlife track those in the atmosphere? – Implications for evaluating the effectiveness of the Minamata Convention. Science of The Total Environment 674, 58–70. https://doi.org/10.1016/j.scitotenv.2019.04.101

Wu, P., Dutkiewicz, S., Monier, E., Zhang, Y., 2021. Bottom-Heavy Trophic Pyramids Impair Methylmercury Biomagnification in the Marine Plankton Ecosystems. Environmental Science & Technology. 55, 15476–15483. https://doi.org/10.1021/acs.est.1c04083

Wu, Y., Wang, W.-X., 2011. Accumulation, subcellular distribution and toxicity of inorganic mercury and methylmercury in marine phytoplankton. Environmental Pollution, Nitrogen Deposition, Critical Loads and Biodiversity 159, 3097–3105. https://doi.org/10.1016/j.envpol.2011.04.012

Yoon, S.-J., Diener, L.M., Bloom, P.R., Nater, E.A., Bleam, W.F., 2005. X-ray absorption

studies of CH3Hg+-binding sites in humic substances. Geochimica et Cosmochimica Acta 69, 1111–1121. https://doi.org/10.1016/j.gca.2004.07.036

Zhang, Y., Jaeglé L., Thompson L., 2014. Natural biogeochemical cycle of mercury in a global three-dimensional ocean tracer model. Global Biogeochemical Cycles 28, 553–570. https://doi.org/10.1002/2014GB004814

Zhang, Y., Soerensen, A.L., Schartup, A.T., Sunderland, E.M., 2020. A global model for methylmercury formation and uptake at the base of marine food webs. Global Biogeochemical Cycles. https://doi.org/10.1029/2019GB006348

Figure captions

Figure 1: Location of the ten sampling stations of the MERITE-HIPPOCAMPE cruise in the Mediterranean Sea (April-Mai 2019).

Figure 2: Boxplot of the concentrations of A) THg, B) MMHg (ng g^{-1} dw) and C) %MMHg in the different plankton size-fractions (fractions between 0.7 and 20 µm (green scale) and >60 µm (red scale) for all stations combined. H = Kruskal–Wallis nonparametric test and the associated p-value for the respective Hg species (H = 24, $p < 0.0001$; H = 36, $p < 0.0001$ and H = 30, $p < 0.0001$, respectively). The mean and median values are represented by a cross and a horizontal line, respectively, and the box length is defined as the interquartile range. The minimum and maximum values are represented by whiskers. Mean values with different post-hoc letters are significantly different ($p < 0.05$).

Figure 3: Logarithm of THg (A) and MMHg (B) concentrations in function of $\delta^{15}N$ (‰) in the different phyto- (green dots) and zooplankton (red dots) size-fractions. The linear regression curve with its equation and the R-square are indicated.

Figure 4: Transfer efficiency between phytoplankton (0.7 to 20 µm fractions) and zooplankton (>60 µm fractions) amounts of THg (A) and MMHg (B) (in pg m^{-3}) by station. Yellow, orange and red isolines represent transfer efficiencies of 1, 5 and 10% for THg and 10, 50 and 100% for MMHg, respectively.

Figure 5: Box plots of A) THg (yellow) and B) MMHg (red) (in ng g^{-1} dw) concentrations measured in the 60 to 1000 µm zooplankton size-fractions by station. The mean and median values are represented by a cross and a horizontal line, respectively, and the box length is defined as the interquartile range.

Figure 6: Trophic magnification factors of THg (TMF_{THg}, in yellow) and MMHg (TMF_{MMHg} in red) at the different stations. >1 values indicated biomagnification, while <1 indicated bioreduction.

Figures

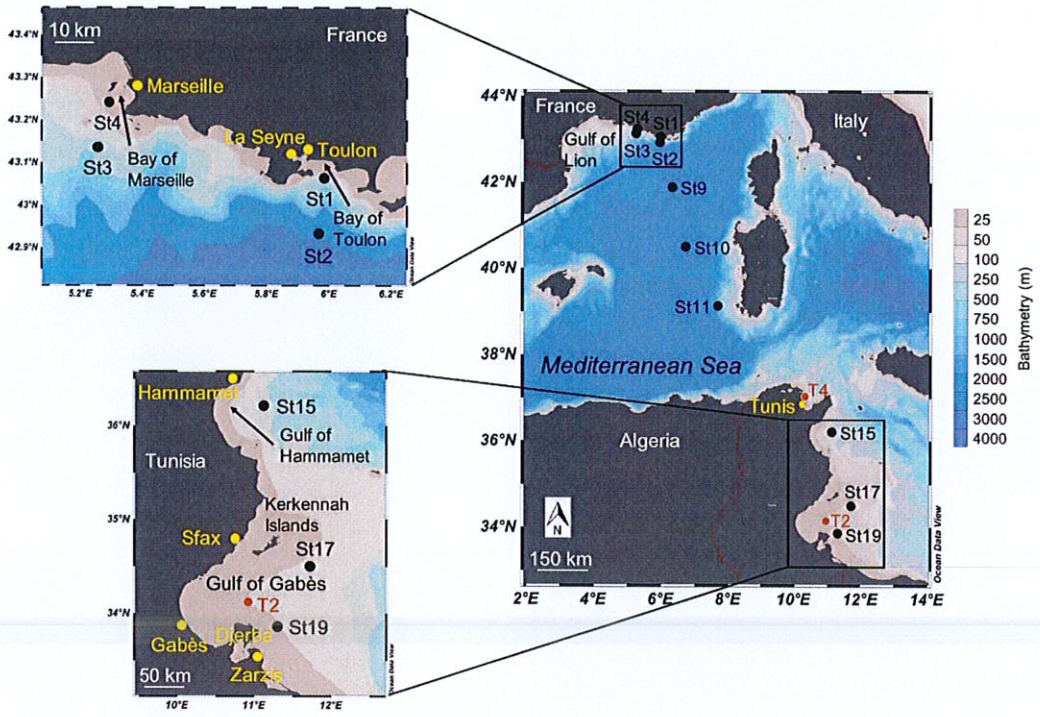

Figure 1

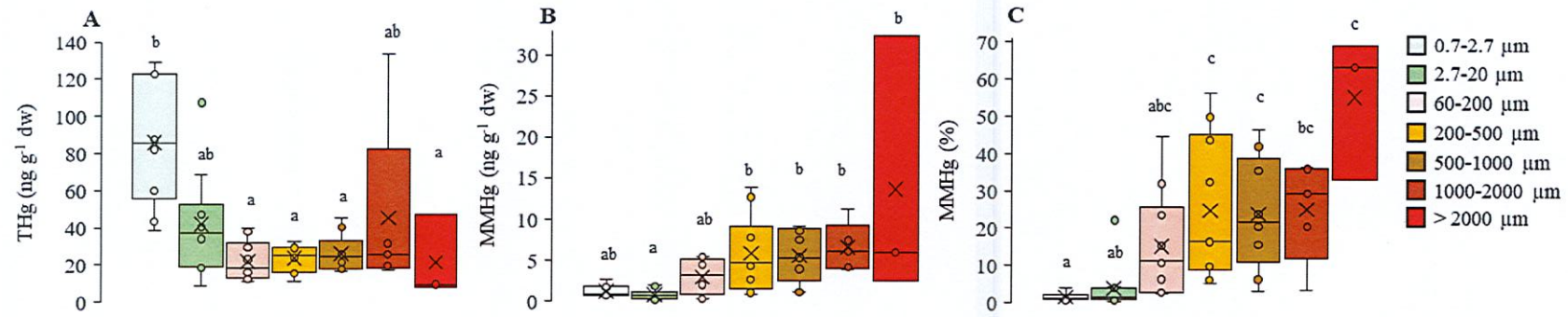
A
B
C
THg (ng g-1 dw)
MMHg (ng g-1 dw)
MMHg (%)
0.7-2.7 µm
2.7-20 µm
60-200 µm
200-500 µm
500-1000 µm
1000-2000 µm
> 2000 µm

Figure 2

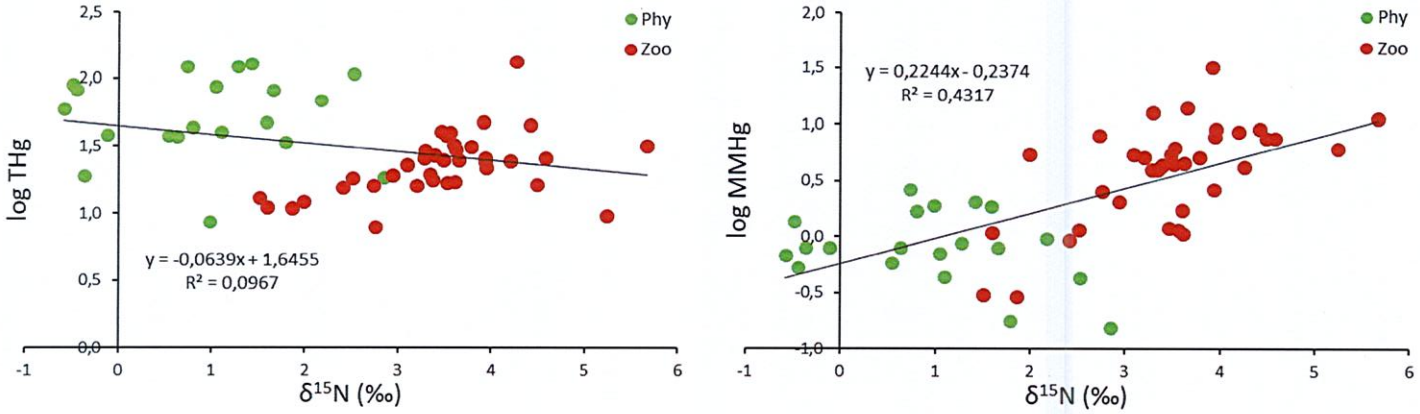
Phy
Zoo
log THg
y = -0,0639x + 1,6455
R² = 0,0967
δ15N (‰)
log MMHg
y = 0,2244x - 0,2374
R² = 0,4317
δ15N (‰)

Figure 3

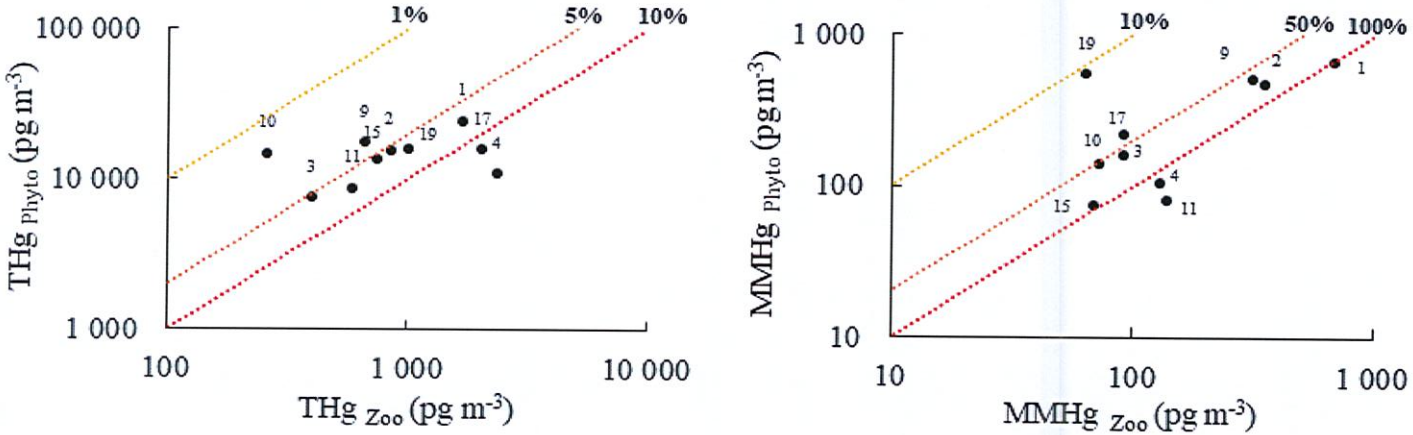

Figure 4

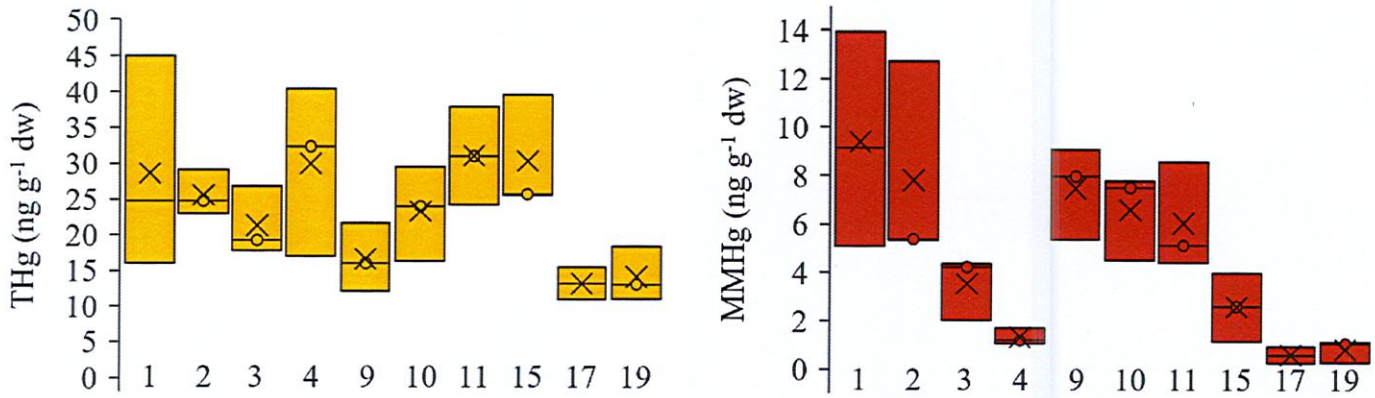
THg (ng g-1 dw)
50
45
40
35
30
25
20
15
10
5
0
1 2 3 4 9 10 11 15 17 19
MMHg (ng g-1 dw)
14
12
10
8
6
4
2
0
1 2 3 4 9 10 11 15 17 19

Figure 5

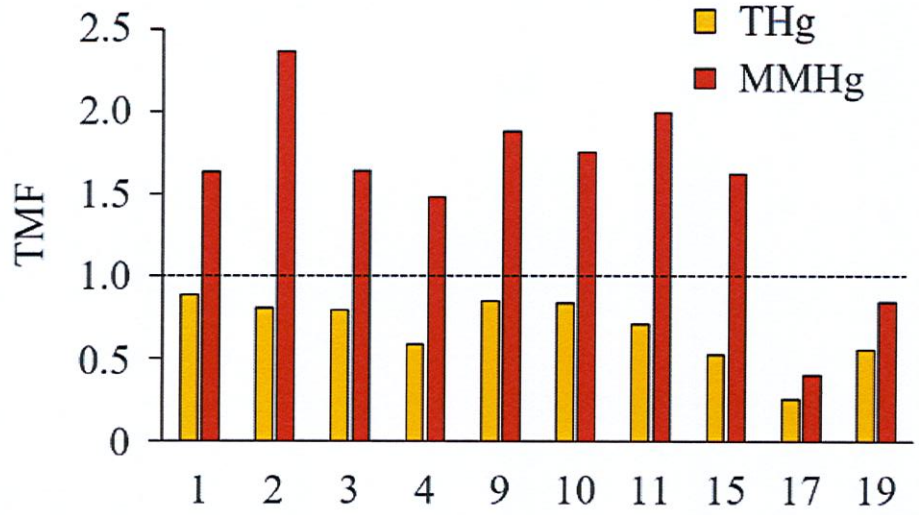

1143

1144 **Figure 6**

Supplementary information

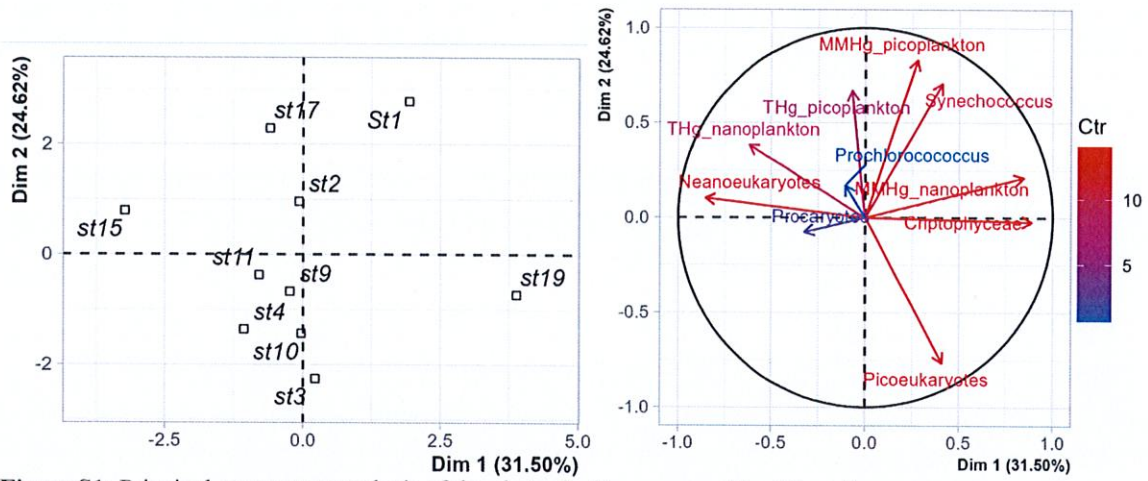

Figure S1: Principal component analysis of the phytoplankton composition (*Synechococcus* spp., *Prochlorococcus* spp., picoeukaryotes, nanoeukaryotes and cryptophyceae), THg and MMHg in the 0.7–2.7 and 2.7–20 µm size-fractions by station. Color gradient indicates the contribution of the variables from blue for low contribution to red for high contribution.

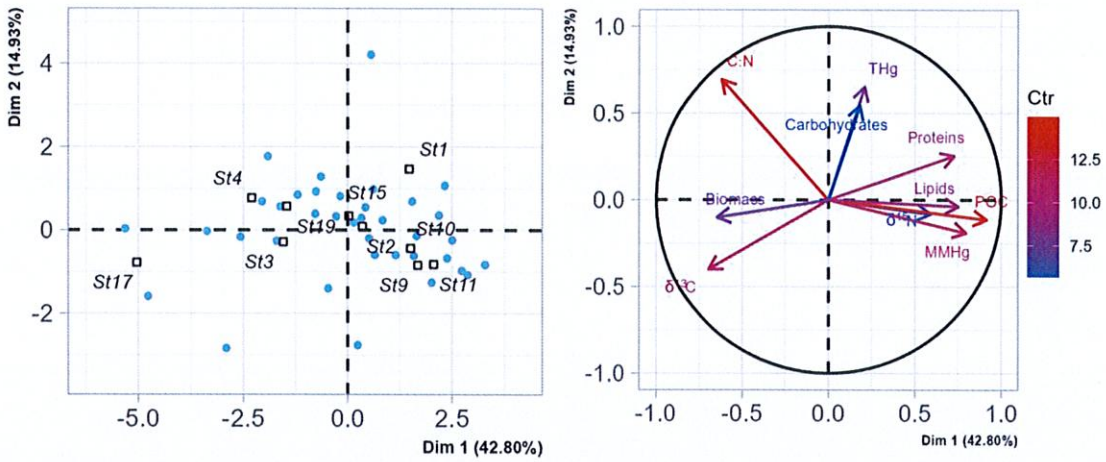

Figure S2: Principal component analysis of the biochemical variables (zooplankton biomass, $\delta^{13}C$, $\delta^{15}N$, C/N, POC, proteins, carbohydrates and lipids), THg and MMHg in zooplankton (60 to 1000 µm fractions) by station. Color gradient indicates the contribution of the variables from blue for low contribution to red for high contribution.

Table S1. Main characteristics of the ten sampling stations of the MERITE-HIPPOCAMPE cruise (13 April–14 May 2019) aboard the R/V *Antea* along a north-south transect in the Mediterranean Sea. The environmental conditions in these stations were detailed in Tedetti et al. (2023).

Station	Location	Latitude (N)	Longitude (E)	Bottom depth (m)	McLane sampling depth (m)	MultiNet sampling depth (m)
St1	Bay of Toulon (north)	43° 03.819'	5° 59.080'	91	20	20
St2	Toulon - Anthares (north)	42° 56.020'	5° 58.041'	1770	25	34
St3	Marseille - Julio (north)	43° 08.150'	5° 15.280'	95	55	58
St4	Bay of Marseille (north)	43° 14.500'	5° 17.500'	58	31	35
St9	North Balearic Front (offshore)	41° 53.508'	6° 19.998'	2575	20	20
St10	North Balearic Front (offshore)	40° 18.632'	7° 14.753'	2791	50	30
St11	North Balearic Front (offshore)	39° 07.998'	7° 41.010'	1378	40	30
St15	Gulf of Hammamet (south)	36° 12.883'	11° 07.641'	100	40	60
St17	Gulf of Gabès (south)	34° 30.113'	11° 43.573'	50	40	40